Interaction Notes

Note 575

30 April 2002

A Finite-Difference-Time-Domain/Perfectly-Matched-Layer Algorithm Applied For Nonlinear Dispersive Media[†]

S. J. Yakura
Air Force Research Laboratory
Directed Energy Directorate

Abstract

The Perfectly-Matched-Layer (PML) method is used to absorb outgoing electromagnetic waves in Finite-Difference-Time-Domain (FDTD) numerical simulations to create the notion of infinity within the finite numerical volume. Starting with the unsplit-field, uniaxial PML formulation, a three-dimensional, second-order FDTD/PML algorithm is obtained for the first time using the piecewise-linear approximation for nonlinear dispersive media. In the absence of the PML interface, the FDTD/PML algorithm reduces to the usual nonlinear, dispersive FDTD/nonPML algorithm. For numerical validation a one-dimensional FDTD/PML demonstration is carried out for an ultra-short electromagnetic pulse propagating inside a nonlinear Raman scattering medium with the PML absorbing boundary condition to show the efficient absorption of outgoing waves.

[†]This work was sponsored in part by the Air Force Office of Scientific Research, and in part by the Air Force Research Laboratory, Directed Energy Directorate, Kirtland AFB, NM 87117 USA

TABLE OFCONTENTS

LIST OF FIGURES

I. INTRODUCTION

With the advent of high power computers that provide fast execution times and great quantities of computer memory, we are at the stage where we can perform direct numerical calculations of Maxwell's equations in nonlinear dispersive materials. Out of many numerical techniques available in the computational electromagnetics community, one that has shown great promise in the time domain is the well-known finite-difference-time-domain (FDTD) method.[1] It is based on using a simple staggered differencing scheme in both time and space to calculate the transient behavior of electromagnetic field quantities. One of the greatest challenges of the FDTD methods has been the efficient and accurate formulation of electromagnetic wave interactions in unbounded regions. For those problems, an absorbing boundary condition must be introduced at the outer layer boundary to simulate the extension of the lattice to infinity. One approach that has given great promise in realizing such an absorbing outer boundary inside the finite volume computational domain is the well-known perfectly-matched-layer (PML) algorithm that was first introduced by J. P. Berenger[2] in 1994 for the free space boundary. Since that time Chew and Weedon[3] came up with the modified PML algorithm that is based on complex coordinate stretching, which is shown to be equivalent to the anisotropic PML medium approach introduced by Sacks *et al.*[4]

In this paper, we explore the formulation of a three-dimensional PML algorithm used to describe the behavior of electromagnetic quantities in outer absorbing boundary layers of a nonlinear dispersive medium that serves to absorb all outgoing waves within a finite computational volume. We consider the case where the electromagnetic wave propagates outwardly from a nonlinear dispersive medium to a nonlinear dispersive PML medium through a reflectionless PML interface. We start the analysis based on the extension of the unsplit-field, uniaxial PML formulation[4-8] of Maxwell's equations that are obtained in the frequency domain inside the nonlinear dispersive PML medium. We perform the inverse Fourier transform of these equations from the frequency domain to the time domain in order to obtain a set of first-order differential equations. Then, these equations are finite differenced in both time and space using the usual staggered Yee FDTD scheme[1] while expanding the electric and magnetic field vectors in time using a Taylor series about the current time step to evaluate next time step values of the electromagnetic field quantities. Depending on the number of terms kept in the Taylor series expansion, we can numerically update the field values to any desired accuracy in time. In Section II, we use the piecewise-linear approximation, which is equivalent to keeping only the first-order, time-dependent term of a Taylor series, to show the process involved in obtaining a second-order accurate FDTD/PML algorithm. To obtain higher-order accurate FDTD/PML algorithms in time, we simply need to include higher-order, time-dependent terms of the Taylor series expansion and follow the same procedure outlined in Section II. In the absence of the PML interface, the FDTD/PML algorithm is shown to reduce to the known FDTD algorithm for nonlinear dispersive media.[9] In Section III, we show the actual one-dimensional numerical demonstration of our FDTD/PML algorithm for an ultra-short electromagnetic pulse propagating inside a nonlinear Raman scattering medium with the nonlinear PML absorbing boundary condition to show the efficient absorption of outgoing waves. Finally, Section IV gives concluding remarks.

II. PML FORMULATION FOR NONLINEAR DISPERSIVE MEDIA

For a wave propagating into anisotropic, uniaxial nonlinear dispersive PML media, the modified Maxwell equations under the unsplit-field, uniaxial anisotropic PML formulation[4] can be expressed in the frequency domain as ($e^{j\omega t}$ convention)

$$\underline{\nabla} \times \underline{\tilde{E}}(\omega;\underline{x}) = -j\omega\, \underline{\underline{\tilde{S}}}^{PML}(\omega) \bullet \mu_0\mu_R\, \underline{\tilde{H}}(\omega;\underline{x}), \tag{2.1}$$

$$\underline{\nabla} \times \underline{\tilde{H}}(\omega;\underline{x}) = j\omega\, \underline{\underline{\tilde{S}}}^{PML}(\omega) \bullet \underline{\tilde{D}}(\omega;\underline{x}), \tag{2.2}$$

with

$$\underline{\tilde{D}}(\omega;\underline{x}) = \varepsilon_0\varepsilon_R\underline{\tilde{E}}(\omega;\underline{x}) + \varepsilon_0\sum_{\rho=1}^{\rho_{max}}\underline{\tilde{P}}_\rho^{L}(\omega;\underline{x}) + \varepsilon_0\sum_{\rho=1}^{\rho_{max}}\underline{\tilde{P}}_\rho^{NL}(\omega;\underline{x}), \tag{2.3}$$

$$\underline{\tilde{P}}_{\rho}^{L}(\omega;\underline{x}) = \mathcal{F}\left\{\underline{P}_{\rho}^{L}(t;\underline{x})\right\} \equiv \mathcal{F}\left\{\int_{-\infty}^{t} d\tau\, X_{\rho}^{L}(t-\tau)\,\underline{E}(\tau;\underline{x})\right\} = X_{\rho}^{L}(\omega)\,\underline{\tilde{E}}(\omega;\underline{x}), \tag{2.4}$$

$$\underline{\tilde{P}}_{\rho}^{NL}(\omega;\underline{x}) = \mathcal{F}\left\{\underline{E}(t;\underline{x})\, R_{\rho}^{NL}(t;\underline{x})\right\} \equiv \mathcal{F}\left\{\underline{E}(t;\underline{x}) \int_{-\infty}^{t} d\tau\, X_{\rho}^{NL}(t-\tau)\,[\underline{E}(\tau;\underline{x}) \bullet \underline{E}(\tau;\underline{x})]\right\}, \tag{2.5}$$

where $\underline{\tilde{E}}(\omega;\underline{x})$ is the complex electric field vector, $\underline{\tilde{H}}(\omega;\underline{x})$ is the complex magnetic field vector, $\underline{\tilde{D}}(\omega;\underline{x})$ is the complex displacement field vector, $\underline{\tilde{P}}_{\rho}^{L}(\omega;\underline{x})$ is the complex linear (first-order) electric polarization vector, $\underline{\tilde{P}}_{\rho}^{NL}(\omega;\underline{x})$ is the complex nonlinear (third-order) electric polarization vector, $\underline{\underline{\tilde{S}}}^{PML}(\omega)$ is the complex uniaxial anisotropic PML matrix, ε_o is the free space electric permittivity, ε_R is the relative permittivity of a medium at infinite frequency, μ_0 is the free-space permeability, μ_R is the relative permeability, $X_{\rho}^{L}(t)$ and $X_{\rho}^{NL}(t)$ are the ρ^{th} terms of the collection consisting of ρ_{max} time-dependent linear and nonlinear electric susceptibility functions, where ρ_{max} is the maximum number of terms which we choose to consider for a particular formulation of (2.3). In (2.5) $R_{\rho}^{NL}(t;\underline{x})$ is introduced to isolate the part of $\underline{\tilde{P}}_{\rho}^{NL}(\omega;\underline{x})$ that is represented by a convolution function. In the above equations, we use notations $\bullet$ and $\mathcal{F}\{\ \}$ to denote, respectively, a vector dot product and the Fourier transform operation. We also use symbol $\sim$ above functions to denote ω-dependence in order to distinguish them from time-dependent functions. Elements of the uniaxial anisotropic PML matrix, $\underline{\underline{\tilde{S}}}^{PML}(\omega)$, are given by[6]

$$\underline{\underline{\tilde{S}}}^{PML}(\omega) = \text{diag}\left\{\frac{\tilde{S}_y(\omega)\,\tilde{S}_z(\omega)}{\tilde{S}_x(\omega)}, \frac{\tilde{S}_z(\omega)\,\tilde{S}_x(\omega)}{\tilde{S}_y(\omega)}, \frac{\tilde{S}_x(\omega)\,\tilde{S}_y(\omega)}{\tilde{S}_z(\omega)}\right\}, \tag{2.6}$$

where "diag" is used to represent diagonal terms of a matrix, and $\tilde{S}_x(\omega)$, $\tilde{S}_y(\omega)$ and $\tilde{S}_z(\omega)$ are ω-dependent functions that satisfy the impedance matching condition at the interface of the non-PML medium and the PML medium. It is a common practice in the computational electromagnetics community to choose $\tilde{S}_x(\omega)$, $\tilde{S}_y(\omega)$ and $\tilde{S}_z(\omega)$ as

$$\tilde{S}_x(\omega) = 1 + \frac{\sigma_x}{j\omega\varepsilon_o} \quad \text{with} \quad \frac{\sigma_x}{\varepsilon_o} = \frac{\sigma_x^*}{\mu_o}, \tag{2.7-2.8}$$

$$\tilde{S}_y(\omega) = 1 + \frac{\sigma_y}{j\omega\varepsilon_o} \quad \text{with} \quad \frac{\sigma_y}{\varepsilon_o} = \frac{\sigma_y^*}{\mu_o}, \tag{2.9-2.10}$$

$$\tilde{S}_z(\omega) = 1 + \frac{\sigma_z}{j\omega\varepsilon_o} \quad \text{with} \quad \frac{\sigma_z}{\varepsilon_o} = \frac{\sigma_z^*}{\mu_o}, \tag{2.11-2.12}$$

where σ_x, σ_y and σ_z are PML electric conductivities, and σ_x^*, σ_y^* and σ_z^* are PML magnetic conductivities with subscripts x, y and z denoting the directions in which PML conductivities are assigned[2]. These PML conductivities are introduced for the purpose of properly handling the impedance matching condition at the nonPML/PML interface.

We first eliminate $\underline{\tilde{D}}(\omega;\underline{x})$ in favor of expressing Maxwell's equations in terms of $\underline{\tilde{E}}(\omega;\underline{x})$, $\underline{\tilde{P}}_{\rho}^{L}(\omega;\underline{x})$ and $\underline{\tilde{P}}_{\rho}^{NL}(\omega;\underline{x})$ by substituting (2.3) into (2.2). Then, taking the inverse Fourier transforms of (2.1), (2.2), (2.4) and (2.5) directly based on the delayed axial field convolution technique[10] with expressions shown in (2.7) through (2.12), we obtain the following time-dependent equations:

$$\mu_0\mu_R\frac{\partial \underline{H}(t;\underline{x})}{\partial t}+\mu_0\mu_R\underline{\underline{\Xi}}_0\bullet\underline{H}(t;\underline{x})+\mu_0\mu_R\underline{\underline{\Xi}}_1\bullet\underline{H}^{Delay}(t;\underline{x})+\underline{\nabla}\times\underline{E}(t;\underline{x})=0\,, \tag{2.13}$$

$$\begin{aligned}\varepsilon_0\varepsilon_R\frac{\partial \underline{E}(t;\underline{x})}{\partial t}&+\varepsilon_0\sum_\rho\frac{\partial \underline{P}_\rho^{L}(t;\underline{x})}{\partial t}+\varepsilon_0\sum_\rho\frac{\partial[\underline{E}(t;\underline{x})\,R_\rho^{NL}(t;\underline{x})]}{\partial t}\\&+\varepsilon_0\underline{\underline{\Xi}}_0\bullet\Big[\varepsilon_R\underline{E}(t;\underline{x})+\sum_\rho\underline{P}_\rho^{L}(t;\underline{x})+\underline{E}(t;\underline{x})\sum_\rho R_\rho^{NL}(t;\underline{x})\Big]\\&+\varepsilon_0\underline{\underline{\Xi}}_1\bullet\Big[\varepsilon_R\underline{E}^{Delay}(t;\underline{x})+\sum_\rho\underline{P}_\rho^{LDelay}(t;\underline{x})+\sum_\rho\underline{P}_\rho^{NLDelay}(t;\underline{x})\Big]-\underline{\nabla}\times\underline{H}(t;\underline{x})=0\,,\end{aligned} \tag{2.14}$$

with

$$\underline{P}_\rho^{L}(t;\underline{x})=\int_{-\infty}^{t}d\tau\,X_\rho^{L}(t-\tau)\,\underline{E}(\tau;\underline{x})\,, \tag{2.15}$$

$$R_\rho^{NL}(t;\underline{x})=\int_{-\infty}^{t}d\tau\,X_\rho^{NL}(t-\tau)\,[\underline{E}(\tau;\underline{x})\bullet\underline{E}(\tau;\underline{x})]\,, \tag{2.16}$$

$$\underline{H}^{Delay}(t;\underline{x})=\int_{-\infty}^{t}d\tau\,\underline{\underline{\Phi}}(t-\tau)\bullet\underline{H}(\tau;\underline{x})\,, \tag{2.17}$$

$$\underline{E}^{Delay}(t;\underline{x})=\int_{-\infty}^{t}d\tau\,\underline{\underline{\Phi}}(t-\tau)\bullet\underline{E}(\tau;\underline{x})\,, \tag{2.18}$$

$$\underline{P}_\rho^{LDelay}(t;\underline{x})=\int_{-\infty}^{t}d\tau\,\underline{\underline{\Phi}}(t-\tau)\bullet\underline{P}_\rho^{L}(\tau;\underline{x})\,, \tag{2.19}$$

$$\underline{P}_\rho^{NLDelay}(t;\underline{x})=\int_{-\infty}^{t}d\tau\,\underline{\underline{\Phi}}(t-\tau)\bullet[\underline{E}(\tau;\underline{x})\,R_\rho^{NL}(\tau;\underline{x})]\,, \tag{2.20}$$

where

$$\underline{\underline{\Xi}}_0=\mathrm{diag}\,\{(\frac{\sigma_y}{\varepsilon_0}+\frac{\sigma_z}{\varepsilon_0}-\frac{\sigma_x}{\varepsilon_0}),(\frac{\sigma_x}{\varepsilon_0}+\frac{\sigma_z}{\varepsilon_0}-\frac{\sigma_y}{\varepsilon_0}),(\frac{\sigma_x}{\varepsilon_0}+\frac{\sigma_y}{\varepsilon_0}-\frac{\sigma_z}{\varepsilon_0})\}\,, \tag{2.21}$$

$$\underline{\underline{\Xi}}_1=\mathrm{diag}\{(\frac{\sigma_y}{\varepsilon_0}-\frac{\sigma_x}{\varepsilon_0})(\frac{\sigma_z}{\varepsilon_0}-\frac{\sigma_x}{\varepsilon_0}),(\frac{\sigma_x}{\varepsilon_0}-\frac{\sigma_y}{\varepsilon_0})(\frac{\sigma_z}{\varepsilon_0}-\frac{\sigma_y}{\varepsilon_0}),(\frac{\sigma_x}{\varepsilon_0}-\frac{\sigma_z}{\varepsilon_0})(\frac{\sigma_y}{\varepsilon_0}-\frac{\sigma_z}{\varepsilon_0})\}\,, \tag{2.22}$$

$$\underline{\underline{\Phi}}(t-\tau)=\mathrm{diag}\{\exp[-(\frac{\sigma_x}{\varepsilon_0})(t-\tau)],\exp[-(\frac{\sigma_y}{\varepsilon_0})(t-\tau)],\exp[-(\frac{\sigma_z}{\varepsilon_0})(t-\tau)]\}\,. \tag{2.23}$$

In the above, $\underline{H}^{Delay}(t;\underline{x})$, $\underline{E}^{Delay}(t;\underline{x})$, $\underline{P}_\rho^{LDelay}(t;\underline{x})$ and $\underline{P}_\rho^{NLDelay}(t;\underline{x})$ are introduced to handle the delayed time-response behavior of $\underline{H}(t;\underline{x})$, $\underline{E}(t;\underline{x})$, $\underline{P}_\rho^{L}(t;\underline{x})$ and $[\underline{E}(t;\underline{x})R_\rho^{NL}(t;\underline{x})]$, respectively. These functions follow naturally from taking the inverse Fourier transforms of convolution functions $[1/(j\omega\,\underline{\underline{I}}+\underline{\underline{A}})]\,\underline{\tilde{H}}(\omega;\underline{x})$, $[1/(j\omega\,\underline{\underline{I}}+\underline{\underline{A}})]\,\underline{\tilde{E}}(\omega;\underline{x})$, $[1/(j\omega\,\underline{\underline{I}}+\underline{\underline{A}})]\,\underline{\tilde{P}}_\rho^{L}(\omega;\underline{x})$ and $[1/(j\omega\,\underline{\underline{I}}+\underline{\underline{A}})]\,\underline{\tilde{P}}_\rho^{NL}(\omega;\underline{x})$ by realizing the fact that the inverse Fourier transform of $[1/(j\omega\,\underline{\underline{I}}+\underline{\underline{A}})]$ which transforms back to the time domain is simply given by $\exp(-\underline{\underline{A}}\,t)$, where $\underline{\underline{I}}$ is the identity matrix and $\underline{\underline{A}}$ is a time independent diagonal matrix expressed as $\mathrm{diag}\{(\sigma_x/\varepsilon_0),(\sigma_y/\varepsilon_0),(\sigma_z/\varepsilon_0)\}$.

To solve (2.13) through (2.20), we need to specify expressions for linear and nonlinear electric susceptibility functions. In this paper we consider the general case in which both the linear and nonlinear electric susceptibility functions are expressed as complex functions that contain complex coefficients and exhibit exponential behavior in the time domain as follows:

$$X_\rho^{L}(t)=\mathrm{Re}\,\{\alpha_\rho^{L}\exp[-(\gamma_\rho^{L})t]\}\,U(t)\,, \tag{2.24}$$

$$\chi_\rho^{NL}(t) = \mathrm{Re}\,\{\alpha_\rho^{NL}\exp[-(\gamma_\rho^{NL})t]\}\,U(t)\,, \tag{2.25}$$

where Re{ } is used to represent the real part of a complex function, U(t) is the unit step function, and α_ρ^L, γ_ρ^L, α_ρ^{NL} and γ_ρ^{NL} are complex coefficients. We need to point out that by making the proper choices of complex coefficients and performing the Fourier transforms of (2.24) and (2.25), one can obtain the familiar forms of the complex permittivity in the frequency domain for the constant conductivity [i.e., by setting α_ρ^L to be a real number, $\gamma_\rho^L = 0$, $\alpha_\rho^{NL} = 0$ and $\gamma_\rho^{NL} = 0$], the Debye model [i.e., by setting α_ρ^L, γ_ρ^L, α_ρ^{NL} and γ_ρ^{NL} to be all real numbers] and the Lorentz model [i.e., by setting α_ρ^L and α_ρ^{NL} to be both imaginary numbers, and γ_ρ^L and γ_ρ^{NL} to be both complex numbers].

Upon substituting (2.24) and (2.25) into (2.15) and (2.16), we obtain the following expressions for $\underline{P}_\rho^{\,L}(t;\underline{x})$ and $R_\rho^{NL}(t;\underline{x})$:

$$\underline{P}_\rho^{L}(t;\underline{x}) \equiv \mathrm{Re}\,\{\underline{Q}_\rho^{L}(t;\underline{x})\} = \mathrm{Re}\,\{\alpha_\rho^L \int_{-\infty}^{t} d\tau\,\exp[-(\gamma_\rho^L)(t-\tau)]\,\underline{E}(\tau;\underline{x})\}\,, \tag{2.26}$$

$$R_\rho^{NL}(t;\underline{x}) \equiv \mathrm{Re}\,\{Q_\rho^{NL}(t;\underline{x})\} = \mathrm{Re}\,\{\alpha_\rho^{NL} \int_{-\infty}^{t} d\tau\,\exp[-(\gamma_\rho^{NL})(t-\tau)]\,[\underline{E}(\tau;\underline{x})\bullet\underline{E}(\tau;\underline{x})]\}\,, \tag{2.27}$$

where complex functions, $\underline{Q}_\rho^{\,L}(t;\underline{x})$ and $Q_\rho^{NL}(t;\underline{x})$, are introduced in the above equations such that the real parts of these complex functions result in $\underline{P}_\rho^{\,L}(t;\underline{x})$ and $R_\rho^{NL}(t;\underline{x})$, respectively.

To derive FDTD expressions based on the staggered Yee scheme,[1] (2.13), (2.14), (2.25), (2,26) and (2.17) through (2.20) have to be solved numerically for $\underline{H}(t;\underline{x})$, $\underline{E}(t;\underline{x})$, $\underline{Q}_\rho^{\,L}(t;\underline{x})$, $Q_\rho^{NL}(t;\underline{x})$, $\underline{H}^{Delay}(t;\underline{x})$, $\underline{E}^{Delay}(t;\underline{x})$, $\underline{P}_\rho^{\,LDelay}(t;\underline{x})$ and $\underline{P}_\rho^{\,NLDelay}(t;\underline{x})$ at each time step by correctly carrying out the numerical integration of convolution integrals $\underline{Q}_\rho^{\,L}(t;\underline{x})$, $Q_\rho^{NL}(t;\underline{x})$, $\underline{H}^{Delay}(t;\underline{x})$, $\underline{E}^{Delay}(t;\underline{x})$, $\underline{P}_\rho^{\,LDelay}(t;\underline{x})$ and $\underline{P}_\rho^{\,NLDelay}(t;\underline{x})$. Therefore, the whole solution rests on the question of how to carry out the numerical integration of $\underline{Q}_\rho^{\,L}(t;\underline{x})$, $Q_\rho^{NL}(t;\underline{x})$, $\underline{H}^{Delay}(t;\underline{x})$, $\underline{E}^{Delay}(t;\underline{x})$, $\underline{P}_\rho^{\,LDelay}(t;\underline{x})$ and $\underline{P}_\rho^{\,NLDelay}(t;\underline{x})$ at each time step. For that reason, the rest of this section is devoted to the numerical formulation that treats $\underline{Q}_\rho^{\,L}(t;\underline{x})$, $Q_\rho^{NL}(t;\underline{x})$, $\underline{H}^{Delay}(t;\underline{x})$, $\underline{E}^{Delay}(t;\underline{x})$, $\underline{P}_\rho^{\,LDelay}(t;\underline{x})$ and $\underline{P}_\rho^{\,NLDelay}(t;\underline{x})$ into the overall FDTD scheme based on the recursive convolution approach.[9]

We first convert the convolution integrals $\underline{Q}_\rho^{\,L}(t;\underline{x})$, $Q_\rho^{NL}(t;\underline{x})$, $\underline{H}^{Delay}(t;\underline{x})$, $\underline{E}^{Delay}(t;\underline{x})$, $\underline{P}_\rho^{\,LDelay}(t;\underline{x})$ and $\underline{P}_\rho^{\,NLDelay}(t;\underline{x})$ into the following equivalent first-order differential equations:

$$\frac{\partial \underline{Q}_\rho^{L}(t;\underline{x})}{\partial t} + (\gamma_\rho^L)\,\underline{Q}_\rho^{L}(t;\underline{x}) = \alpha_\rho^L\,\underline{E}(t;\underline{x})\,, \tag{2.28}$$

$$\frac{\partial Q_\rho^{NL}(t;\underline{x})}{\partial t} + (\gamma_\rho^{NL})\,Q_\rho^{NL}(t;\underline{x}) = \alpha_\rho^{NL}\,[\underline{E}(t;\underline{x})\bullet\underline{E}(t;\underline{x})]\,, \tag{2.29}$$

$$\frac{\partial \underline{H}^{Delay}(t;\underline{x})}{\partial t} + \underline{\underline{\Phi}}(t)\bullet\underline{H}^{Delay}(t;\underline{x}) = \underline{H}(t;\underline{x})\,, \tag{2.30}$$

$$\frac{\partial \underline{E}^{Delay}(t;\underline{x})}{\partial t} + \underline{\underline{\Phi}}(t)\bullet\underline{E}^{Delay}(t;\underline{x}) = \underline{E}(t;\underline{x})\,, \tag{2.31}$$

$$\frac{\partial \underline{Q}_\rho^{LDelay}(t;\underline{x})}{\partial t} + \underline{\underline{\Phi}}(t)\bullet\underline{Q}_\rho^{LDelay}(t;\underline{x}) = \underline{Q}_\rho^{L}(t;\underline{x})\,, \tag{2.32}$$

$$\frac{\partial \underline{Q}_\rho^{NLDelay}(t;\underline{x})}{\partial t} + \underline{\underline{\Phi}}(t) \bullet \underline{Q}_\rho^{NLDelay}(t;\underline{x}) = \underline{E}(t;\underline{x})\, Q_\rho^{NL}(t;\underline{x}), \tag{2.33}$$

where complex functions $\underline{Q}_\rho^{LDelay}(t;\underline{x})$ and $\underline{Q}_\rho^{NLDelay}(t;\underline{x})$ are introduced in (2.32) and (2.33) such that the real parts of these complex functions result in $\underline{P}_\rho^{LDelay}(t;\underline{x})$ and $\underline{P}_\rho^{NLDelay}(t;\underline{x})$, respectively.

To show how we can use (2.13), (2.14) and (2.28) through (2.33) to come up with a three-dimensional FDTD/PML algorithm for nonlinear dispersive PML media, we integrate (2.13) and (2.30) from $t=(n-½)\Delta t$ to $t=(n+½)\Delta t$, and (2.14), (2.28), (2.29) and (2.31) through (2.33) from $t=n\Delta t$ to $t=(n+1)\Delta t$. Then (2.28) through (2.33) are solved exactly using the integrating factor technique for a given discrete time interval to go forward in time by Δt.

$$\mu_0\mu_R \int_{(n-½)\Delta t}^{(n+½)\Delta t} d\tau \frac{\partial \underline{H}(\tau;\underline{x})}{\partial \tau} + \mu_0\mu_R \underline{\underline{\Xi}}_0 \bullet \int_{(n-½)\Delta t}^{(n+½)\Delta t} d\tau\, \underline{H}(\tau;\underline{x})$$
$$+ \mu_0\mu_R \underline{\underline{\Xi}}_1 \bullet \int_{(n-½)\Delta t}^{(n+½)\Delta t} d\tau\, \underline{H}^{Delay}(\tau;\underline{x}) + \int_{(n-½)\Delta t}^{(n+½)\Delta t} d\tau\, \underline{\nabla} \times \underline{E}(\tau;\underline{x}) = 0, \tag{2.34}$$

$$\varepsilon_0\varepsilon_R \int_{n\Delta t}^{(n+1)\Delta t} d\tau \frac{\partial \underline{E}(\tau;\underline{x})}{\partial \tau} + \varepsilon_0 \mathrm{Re}\Big\{\sum_\rho \int_{n\Delta t}^{(n+1)\Delta t} d\tau \frac{\partial \underline{Q}_\rho^{L}(\tau;\underline{x})}{\partial \tau}\Big\} + \varepsilon_0 \mathrm{Re}\Big\{\sum_\rho \int_{n\Delta t}^{(n+1)\Delta t} d\tau \frac{\partial [\underline{E}(\tau;\underline{x})\, Q_\rho^{NL}(\tau;x)]}{\partial \tau}\Big\}$$
$$+ \varepsilon_0\varepsilon_R \underline{\underline{\Xi}}_0 \bullet \int_{n\Delta t}^{(n+1)\Delta t} d\tau\, \underline{E}(\tau;\underline{x}) + \varepsilon_0 \underline{\underline{\Xi}}_0 \bullet \mathrm{Re}\Big\{\sum_\rho \int_{n\Delta t}^{(n+1)\Delta t} d\tau\, \underline{Q}_\rho^{L}(\tau;\underline{x})\Big\}$$
$$+ \varepsilon_0 \underline{\underline{\Xi}}_0 \bullet \mathrm{Re}\Big\{\sum_\rho \int_{n\Delta t}^{(n+1)\Delta t} d\tau\, \underline{E}(\tau;\underline{x})\, Q_\rho^{NL}(\tau;\underline{x})\Big\} + \varepsilon_0\varepsilon_R \underline{\underline{\Xi}}_1 \bullet \int_{n\Delta t}^{(n+1)\Delta t} d\tau\, \underline{E}^{Delay}(\tau;\underline{x})$$
$$+ \varepsilon_0 \underline{\underline{\Xi}}_1 \bullet \mathrm{Re}\Big\{\sum_\rho \int_{n\Delta t}^{(n+1)\Delta t} d\tau\, \underline{Q}_\rho^{LDelay}(\tau;\underline{x})\Big\} + \varepsilon_0 \underline{\underline{\Xi}}_1 \bullet \mathrm{Re}\Big\{\sum_\rho \int_{n\Delta t}^{(n+1)\Delta t} d\tau\, \underline{Q}_\rho^{NLDelay}(\tau;\underline{x})\Big\}$$
$$- \int_{n\Delta t}^{(n+1)\Delta t} d\tau\, \underline{\nabla} \times \underline{H}(\tau;\underline{x}) = 0, \tag{2.35}$$

$$\underline{Q}_\rho^{L}(n\Delta t + \Delta t;\underline{x}) = \exp[-(\gamma_\rho^{L})\Delta t]\Big[\underline{Q}_\rho^{L}(n\Delta t;\underline{x}) + \alpha_\rho^{L} \int_{n\Delta t}^{(n+1)\Delta t} d\tau \exp[-(\gamma_\rho^{L})(n\Delta t - \tau)]\, \underline{E}(\tau;\underline{x})\Big], \tag{2.36}$$

$$Q_\rho^{NL}(n\Delta t + \Delta t;\underline{x}) = \exp[-(\gamma_\rho^{NL})\Delta t]\Big[Q_\rho^{NL}(n\Delta t;\underline{x})$$
$$+ \alpha_\rho^{NL} \int_{n\Delta t}^{(n+1)\Delta t} d\tau \exp[-(\gamma_\rho^{NL})(n\Delta t - \tau)]\, [\underline{E}(\tau;\underline{x}) \bullet \underline{E}(\tau;\underline{x})]\Big], \tag{2.37}$$

$$\underline{H}^{Delay}(n\Delta t + ½\Delta t;\underline{x}) = \exp(-\underline{\underline{\Phi}}\Delta t) \bullet \Big[\underline{H}^{Delay}(n\Delta t - ½\Delta t;\underline{x})$$
$$+ \int_{(n-½)\Delta t}^{(n+½)\Delta t} d\tau \exp[-\underline{\underline{\Phi}}(n\Delta t - ½\Delta t - \tau)] \bullet \underline{H}(\tau;\underline{x})\Big], \tag{2.38}$$

$$\underline{E}^{Delay}(n\Delta t+\Delta t;\underline{x}) = \exp(-\underline{\underline{\Phi}}\Delta t)\bullet\Big[\,\underline{E}^{Delay}(n\Delta t;\underline{x}) + \int_{n\Delta t}^{(n+1)\Delta t} d\tau\, \exp[-\underline{\underline{\Phi}}(n\Delta t-\tau)]\bullet\underline{E}(\tau;\underline{x})\,\Big], \tag{2.39}$$

$$\begin{aligned}\underline{Q}_\rho^{LDelay}(n\Delta t+\Delta t;\underline{x}) &= \exp(-\underline{\underline{\Phi}}\Delta t)\bullet\Big[\,\underline{Q}_\rho^{LDelay}(n\Delta t;\underline{x}) + \int_{n\Delta t}^{(n+1)\Delta t} d\tau\, \exp[-\underline{\underline{\Phi}}(n\Delta t-\tau)]\bullet\underline{Q}_\rho^{L}(\tau;\underline{x})\,\Big]\\ &= \exp(-\underline{\underline{\Phi}}\Delta t)\bullet\Big[\,\underline{Q}_\rho^{LDelay}(n\Delta t;\underline{x}) + \int_{n\Delta t}^{(n+1)\Delta t} d\tau\, \exp[-\underline{\underline{\Phi}}(n\Delta t-\tau)-\underline{\underline{I}}\,(\gamma_\rho^{L})(\tau-n\Delta t)]\bullet\underline{Q}_\rho^{L}(n\Delta t;\underline{x})\\ &\quad+\alpha_\rho^{L}\int_{n\Delta t}^{(n+1)\Delta t} d\tau\int_{n\Delta t}^{\tau} d\tau'\,\exp[-\underline{\underline{\Phi}}(n\Delta t-\tau)-\underline{\underline{I}}\,(\gamma_\rho^{L})(\tau-\tau')]\bullet\underline{E}(\tau';\underline{x})\,\Big],\end{aligned} \tag{2.40}$$

$$\begin{aligned}\underline{Q}_\rho^{NLDelay}(n\Delta t+\Delta t;\underline{x}) &= \exp(-\underline{\underline{\Phi}}\Delta t)\bullet\Big[\,\underline{Q}_\rho^{NLDelay}(n\Delta t;\underline{x}) + \int_{n\Delta t}^{(n+1)\Delta t} d\tau\, \exp[-\underline{\underline{\Phi}}(n\Delta t-\tau)]\bullet\underline{E}(\tau;\underline{x})\,Q_\rho^{NL}(\tau;\underline{x})\,\Big]\\ &= \exp(-\underline{\underline{\Phi}}\Delta t)\bullet\Big[\,\underline{Q}_\rho^{NLDelay}(n\Delta t;\underline{x})\\ &\quad+\int_{n\Delta t}^{(n+1)\Delta t} d\tau\,\exp[-\underline{\underline{\Phi}}(n\Delta t-\tau)-\underline{\underline{I}}\,(\gamma_\rho^{NL})(\tau-n\Delta t)]\bullet\underline{E}(\tau;\underline{x})\,Q_\rho^{NL}(n\Delta t;\underline{x})\\ &\quad+\alpha_\rho^{NL}\int_{n\Delta t}^{(n+1)\Delta t} d\tau\int_{n\Delta t}^{\tau} d\tau'\,\exp[-\underline{\underline{\Phi}}(n\Delta t-\tau)-\underline{\underline{I}}\,(\gamma_\rho^{NL})(\tau-\tau')]\bullet\underline{E}(\tau;\underline{x})\,[\underline{E}(\tau';\underline{x})\bullet\underline{E}(\tau';\underline{x})]\,\Big].\end{aligned} \tag{2.41}$$

To obtain second-order accuracy in time from a finite differencing technique, $\underline{H}(t;\underline{x})$ and $\underline{E}(t;\underline{x})$ are taken to be piecewise-linear continuous functions over the entire temporal integration range such that $\underline{H}(t;\underline{x})$ and $\underline{E}(t;\underline{x})$ change linearly with respect to time over given discrete time step intervals. It is equivalent to saying that we use only the first-order, time-dependent term of the Taylor series expansion for $\underline{H}(t;\underline{x})$ and $\underline{E}(t;\underline{x})$, respectively, that are expanded in time about the current time step of $t=(n-\frac{1}{2})\Delta t$ for $\underline{H}(t;\underline{x})$ and the current time step of $t=n\Delta t$ for $\underline{E}(t;\underline{x})$. Mathematically, we can express $\underline{H}(t;\underline{x})$ and $\underline{E}(t;\underline{x})$ in the following forms in terms of $(\underline{H})_{ijk}^{n-\frac{1}{2}}$, $(\underline{H})_{ijk}^{n+\frac{1}{2}}$, $(\underline{E})_{ijk}^{n}$ and $(\underline{E})_{ijk}^{n+1}$ where superscripts $n-\frac{1}{2}$, n, $n+\frac{1}{2}$ and n+1 are used to denote discrete time steps at $t=(n-\frac{1}{2})\Delta t$, $t=n\Delta t$, $t=(n+\frac{1}{2})\Delta t$ and $t=(n+1)\Delta t$, respectively. Subscripts are used to denote discrete spatial locations, $\underline{x}=[i\Delta x, j\Delta y, k\Delta z]$ for $\underline{E}(t;\underline{x})$ and $\underline{x}=[(i-\frac{1}{2})\Delta x, (j-\frac{1}{2})\Delta y, (k-\frac{1}{2})\Delta z]$ for $\underline{H}(t;\underline{x})$ with Δx, Δy and Δz being the spatial grid sizes in the x, y and z directions, respectively.

$$\underline{H}(t;\underline{x}) = \begin{cases}(\underline{H})_{ijk}^{n-\frac{1}{2}} + \dfrac{[(\underline{H})_{ijk}^{n+\frac{1}{2}} - (\underline{H})_{ijk}^{n-\frac{1}{2}}]}{\Delta t}[t-(n-\frac{1}{2})\Delta t] + \text{higher order terms}, & \text{for } 0 \le (n-\frac{1}{2})\Delta t \le t \le (n+\frac{1}{2})\Delta t\\ 0, & \text{for } t<0\end{cases} \tag{2.42}$$

$$\underline{E}(t;\underline{x}) = \begin{cases}(\underline{E})_{ijk}^{n} + \dfrac{[(\underline{E})_{ijk}^{n+1} - (\underline{E})_{ijk}^{n}]}{\Delta t}(t-n\Delta t) + \text{higher order terms}, & \text{for } 0 \le n\Delta t \le t \le (n+1)\Delta t\\ 0, & \text{for } t<0\end{cases} \tag{2.43}$$

Although we are not going to investigate higher than second-order accuracy in time in this paper, it is possible to obtain higher-order accurate FDTD algorithms by simply including more terms beyond the first-order, time-dependent term in the above Taylor series expansion.

Now, substituting (2.42) and (2.43) into (2.34) through (2.41) by keeping only the first-order, time dependent term of the above Taylor series expansion, and then performing the time integration from $t=(n-\frac{1}{2})\Delta t$ to $t=(n+\frac{1}{2})\Delta t$ for field values that depend on the magnetic field [i.e., $\underline{H}(t;\underline{x})$ and $\underline{H}^{Delay}(t;\underline{x})$], and from $t=n\Delta t$ to $t=(n+1)\Delta t$ for field values that depend on the electric field [i.e., $\underline{E}(t;\underline{x})$, $\underline{Q}_\rho^{L}(t;\underline{x})$, $\underline{Q}_\rho^{NL}(t;\underline{x})$, $\underline{E}^{Delay}(t;\underline{x})$, $\underline{Q}_\rho^{LDelay}(t;\underline{x})$ and $\underline{Q}_\rho^{NLDelay}(t;\underline{x})$], (2.34) through (2.41) can be manipulated and cast into the following cubic algebraic forms. These expressions are used to update $(\underline{H})_{ijk}^{n+\frac{1}{2}}$, $(\underline{E})_{ijk}^{n+1}$, $(\underline{Q}_\rho^{L})_{ijk}^{n+1}$, $(\underline{Q}_\rho^{NL})_{ijk}^{n+1}$, $(\underline{E}^{Delay})_{ijk}^{n+1}$, $(\underline{H}^{Delay})_{ijk}^{n+\frac{1}{2}}$, $(\underline{Q}_\rho^{LDelay})_{ijk}^{n+1}$ and $(\underline{Q}_\rho^{NLDelay})_{ijk}^{n+1}$ at each time step:

$$\underline{\underline{\Omega}}_0 \bullet (\underline{H})_{ijk}^{n+\frac{1}{2}} + \underline{\underline{\Omega}}_1 \bullet (\underline{H})_{ijk}^{n-\frac{1}{2}} + \underline{\underline{\Omega}}_2 \bullet (\underline{H}^{Delay})_{ijk}^{n-\frac{1}{2}} + \underline{S}_E = 0, \tag{2.44}$$

$$\begin{aligned}
&(\underline{\underline{\Lambda}}_0)_{ijk}^{n} \bullet (\underline{E})_{ijk}^{n+1} + (\underline{\underline{\Lambda}}_1)_{ijk}^{n} \bullet (\underline{E})_{ijk}^{n} + \mathrm{Re}\Big\{\sum_\rho \underline{\underline{\Gamma}}_{\rho,0}^{L} \bullet (\underline{Q}_\rho^{L})_{ijk}^{n}\Big\} + \underline{\underline{\Omega}}_2 \bullet (\underline{E}^{Delay})_{ijk}^{n} \\
&\quad + \underline{\underline{\Omega}}_3 \bullet \mathrm{Re}\Big\{\sum_\rho (\underline{Q}_\rho^{LDelay})_{ijk}^{n}\Big\} + \underline{\underline{\Omega}}_3 \bullet \mathrm{Re}\Big\{\sum_\rho (\underline{Q}_\rho^{NLDelay})_{ijk}^{n}\Big\} \\
&\quad + \mathrm{Re}\Big\{\sum_\rho \underline{\underline{\Gamma}}_{\rho,0}^{NL}\Big\} \bullet (\underline{E})_{ijk}^{n} [(\underline{E})_{ijk}^{n} \bullet (\underline{E})_{ijk}^{n}] + \mathrm{Re}\Big\{\sum_\rho \underline{\underline{\Gamma}}_{\rho,1}^{NL}\Big\} \bullet (\underline{E})_{ijk}^{n} [(\underline{E})_{ijk}^{n} \bullet (\underline{E})_{ijk}^{n+1}] \\
&\quad + \mathrm{Re}\Big\{\sum_\rho \underline{\underline{\Gamma}}_{\rho,2}^{NL}\Big\} \bullet (\underline{E})_{ijk}^{n} [(\underline{E})_{ijk}^{n+1} \bullet (\underline{E})_{ijk}^{n+1}] + \mathrm{Re}\Big\{\sum_\rho \underline{\underline{\Gamma}}_{\rho,3}^{NL}\Big\} \bullet (\underline{E})_{ijk}^{n+1} [(\underline{E})_{ijk}^{n} \bullet (\underline{E})_{ijk}^{n}] \\
&\quad + \mathrm{Re}\Big\{\sum_\rho \underline{\underline{\Gamma}}_{\rho,4}^{NL}\Big\} \bullet (\underline{E})_{ijk}^{n+1} [(\underline{E})_{ijk}^{n} \bullet (\underline{E})_{ijk}^{n+1}] + \mathrm{Re}\Big\{\sum_\rho \underline{\underline{\Gamma}}_{\rho,5}^{NL}\Big\} \bullet (\underline{E})_{ijk}^{n+1} [(\underline{E})_{ijk}^{n+1} \bullet (\underline{E})_{ijk}^{n+1}] \\
&\quad + \underline{S}_H = 0,
\end{aligned} \tag{2.45}$$

$$(\underline{Q}_\rho^{L})_{ijk}^{n+1} = \Theta_{\rho,0}^{L}\left[(\underline{Q}_\rho^{L})_{ijk}^{n} + \Theta_{\rho,1}^{L} (\underline{E})_{ijk}^{n} + \Theta_{\rho,2}^{L} (\underline{E})_{ijk}^{n+1}\right], \tag{2.46}$$

$$\begin{aligned}
(Q_\rho^{NL})_{ijk}^{n+1} = \Theta_{\rho,0}^{NL}\Big[&(Q_\rho^{NL})_{ijk}^{n} + \Theta_{\rho,1}^{NL}[(\underline{E})_{ijk}^{n} \bullet (\underline{E})_{ijk}^{n}] + \Theta_{\rho,2}^{NL}[(\underline{E})_{ijk}^{n} \bullet (\underline{E})_{ijk}^{n+1}] \\
&+ \Theta_{\rho,3}^{NL}[(\underline{E})_{ijk}^{n+1} \bullet (\underline{E})_{ijk}^{n+1}]\Big],
\end{aligned} \tag{2.47}$$

$$(\underline{H}^{Delay})_{ijk}^{n+\frac{1}{2}} = \underline{\underline{\Omega}}_4 \bullet \left[(\underline{H}^{Delay})_{ijk}^{n-\frac{1}{2}} + \underline{\underline{\Omega}}_5 \bullet (\underline{H})_{ijk}^{n-\frac{1}{2}} + \underline{\underline{\Omega}}_6 \bullet (\underline{H})_{ijk}^{n+\frac{1}{2}}\right], \tag{2.48}$$

$$(\underline{E}^{Delay})_{ijk}^{n+1} = \underline{\underline{\Omega}}_4 \bullet \left[(\underline{E}^{Delay})_{ijk}^{n} + \underline{\underline{\Omega}}_5 \bullet (\underline{E})_{ijk}^{n} + \underline{\underline{\Omega}}_6 \bullet (\underline{E})_{ijk}^{n+1}\right], \tag{2.49}$$

$$(\underline{Q}_\rho^{LDelay})_{ijk}^{n+1} = \underline{\underline{\Omega}}_4 \bullet \left[(\underline{Q}_\rho^{LDelay})_{ijk}^{n} + \underline{\underline{\Pi}}_{\rho,0}^{L} \bullet (\underline{Q}_\rho^{L})_{ijk}^{n} + \underline{\underline{\Pi}}_{\rho,1}^{L} \bullet (\underline{E})_{ijk}^{n} + \underline{\underline{\Pi}}_{\rho,2}^{L} \bullet (\underline{E})_{ijk}^{n+1}\right], \tag{2.50}$$

$$\begin{aligned}
(\underline{Q}_\rho^{NLDelay})_{ijk}^{n+1} = \underline{\underline{\Omega}}_4 \bullet \Big[&(\underline{Q}_\rho^{NLDelay})_{ijk}^{n} + (\underline{Q}_\rho^{NL})_{ijk}^{n} \underline{\underline{\Pi}}_{\rho,0}^{NL} \bullet (\underline{E})_{ijk}^{n} + (\underline{Q}_\rho^{NL})_{ijk}^{n} \underline{\underline{\Pi}}_{\rho,1}^{NL} \bullet (\underline{E})_{ijk}^{n+1} \\
&+ \underline{\underline{\Pi}}_{\rho,2}^{NL} \bullet (\underline{E})_{ijk}^{n} [(\underline{E})_{ijk}^{n} \bullet (\underline{E})_{ijk}^{n}] + \underline{\underline{\Pi}}_{\rho,3}^{NL} \bullet (\underline{E})_{ijk}^{n} [(\underline{E})_{ijk}^{n} \bullet (\underline{E})_{ijk}^{n+1}] \\
&+ \underline{\underline{\Pi}}_{\rho,4}^{NL} \bullet (\underline{E})_{ijk}^{n} [(\underline{E})_{ijk}^{n+1} \bullet (\underline{E})_{ijk}^{n+1}] + \underline{\underline{\Pi}}_{\rho,5}^{NL} \bullet (\underline{E})_{ijk}^{n+1} [(\underline{E})_{ijk}^{n} \bullet (\underline{E})_{ijk}^{n}] \\
&+ \underline{\underline{\Pi}}_{\rho,6}^{NL} \bullet (\underline{E})_{ijk}^{n+1} [(\underline{E})_{ijk}^{n} \bullet (\underline{E})_{ijk}^{n+1}] + \underline{\underline{\Pi}}_{\rho,7}^{NL} \bullet (\underline{E})_{ijk}^{n+1} [(\underline{E})_{ijk}^{n+1} \bullet (\underline{E})_{ijk}^{n+1}]\Big],
\end{aligned} \tag{2.51}$$

where $\underline{S}_E$ and $\underline{S}_H$ are given by

$$\underline{S_E} = \begin{pmatrix} \frac{\Delta t}{(\mu_0\mu_R)\Delta y}\left[(E_z)^n_{i(j+\frac{1}{2})k} - (E_z)^n_{i(j-\frac{1}{2})k}\right] - \frac{\Delta t}{(\mu_0\mu_R)\Delta z}\left[(E_y)^n_{ij(k+\frac{1}{2})} - (E_y)^n_{ij(k-\frac{1}{2})}\right] \\ \frac{\Delta t}{(\mu_0\mu_R)\Delta z}\left[(E_x)^n_{ij(k+\frac{1}{2})} - (E_x)^n_{ij(k-\frac{1}{2})}\right] - \frac{\Delta t}{(\mu_0\mu_R)\Delta x}\left[(E_z)^n_{(i+\frac{1}{2})jk} - (E_z)^n_{(i-\frac{1}{2})jk}\right] \\ \frac{\Delta t}{(\mu_0\mu_R)\Delta x}\left[(E_y)^n_{(i+\frac{1}{2})jk} - (E_y)^n_{(i-\frac{1}{2})jk}\right] - \frac{\Delta t}{(\mu_0\mu_R)\Delta y}\left[(E_x)^n_{i(j+\frac{1}{2})k} - (E_x)^n_{i(j-\frac{1}{2})k}\right] \end{pmatrix}, \tag{2.52}$$

$$\underline{S_H} = \begin{pmatrix} -\frac{\Delta t}{(\varepsilon_0\varepsilon_R)\Delta y}\left[(H_z)^{n+\frac{1}{2}}_{i(j+\frac{1}{2})k} - (H_z)^{n+\frac{1}{2}}_{i(j-\frac{1}{2})k}\right] + \frac{\Delta t}{(\varepsilon_0\varepsilon_R)\Delta z}\left[(H_y)^{n+\frac{1}{2}}_{ij(k+\frac{1}{2})} - (H_y)^{n+\frac{1}{2}}_{ij(k-\frac{1}{2})}\right] \\ -\frac{\Delta t}{(\varepsilon_0\varepsilon_R)\Delta z}\left[(H_x)^{n+\frac{1}{2}}_{ij(k+\frac{1}{2})} - (H_x)^{n+\frac{1}{2}}_{ij(k-\frac{1}{2})}\right] + \frac{\Delta t}{(\varepsilon_0\varepsilon_R)\Delta x}\left[(H_z)^{n+\frac{1}{2}}_{(i+\frac{1}{2})jk} - (H_z)^{n+\frac{1}{2}}_{(i-\frac{1}{2})jk}\right] \\ -\frac{\Delta t}{(\varepsilon_0\varepsilon_R)\Delta x}\left[(H_y)^{n+\frac{1}{2}}_{(i+\frac{1}{2})jk} - (H_y)^{n+\frac{1}{2}}_{(i-\frac{1}{2})jk}\right] + \frac{\Delta t}{(\varepsilon_0\varepsilon_R)\Delta y}\left[(H_x)^{n+\frac{1}{2}}_{i(j+\frac{1}{2})k} - (H_x)^{n+\frac{1}{2}}_{i(j-\frac{1}{2})k}\right] \end{pmatrix}. \tag{2.53}$$

$\underline{\underline{(\Lambda_0)}}^n_{ijk}$ and $\underline{\underline{(\Lambda_1)}}^n_{ijk}$ that appear in the first and second terms of (2.45) are updated at each time step with the updated value of $(Q_\rho^{NL})^n_{ijk}$ in order to include the effect of the nonlinear response. Other coefficients and matrices that appear in (2.44) through (2.51) are represented by $\Theta^L_{\rho,0}$, $\Theta^L_{\rho,1}$, $\Theta^L_{\rho,2}$, $\Theta^{NL}_{\rho,0}$, $\Theta^{NL}_{\rho,1}$, $\Theta^{NL}_{\rho,2}$, $\Theta^{NL}_{\rho,3}$, $\underline{\underline{\Omega_0}}$, $\underline{\underline{\Omega_1}}$, $\underline{\underline{\Omega_2}}$, $\underline{\underline{\Omega_3}}$, $\underline{\underline{\Omega_4}}$, $\underline{\underline{\Omega_5}}$, $\underline{\underline{\Omega_6}}$, $\underline{\underline{\Gamma}}^L_{\rho,0}$, $\underline{\underline{\Gamma}}^{NL}_{\rho,0}$, $\underline{\underline{\Gamma}}^{NL}_{\rho,1}$, $\underline{\underline{\Gamma}}^{NL}_{\rho,2}$, $\underline{\underline{\Gamma}}^{NL}_{\rho,3}$, $\underline{\underline{\Gamma}}^{NL}_{\rho,4}$, $\underline{\underline{\Gamma}}^{NL}_{\rho,5}$, $\underline{\underline{\Pi}}^L_{\rho,0}$, $\underline{\underline{\Pi}}^L_{\rho,1}$, $\underline{\underline{\Pi}}^L_{\rho,2}$, $\underline{\underline{\Pi}}^{NL}_{\rho,0}$, $\underline{\underline{\Pi}}^{NL}_{\rho,1}$, $\underline{\underline{\Pi}}^{NL}_{\rho,2}$, $\underline{\underline{\Pi}}^{NL}_{\rho,3}$, $\underline{\underline{\Pi}}^{NL}_{\rho,4}$, $\underline{\underline{\Pi}}^{NL}_{\rho,5}$, $\underline{\underline{\Pi}}^{NL}_{\rho,6}$, $\underline{\underline{\Pi}}^{NL}_{\rho,7}$. These coefficients and matrices can be evaluated at the beginning of the FDTD/PML simulation since they depend only on material properties and Δt. The material properties that are required for the evaluation of these coefficients and matrices are α^L_ρ, γ^L_ρ, α^{NL}_ρ, γ^{NL}_ρ, σ_x, σ_y and σ_z, which are known quantities since they are assigned for a specific FDTD/PML simulation problem. Shown in Appendix are the explicit expressions of these coefficients and matrices found in (2.44) through (2.51).

Using the above FDTD/PML algorithm the computer simulation can be performed for electromagnetic waves that propagate inside nonlinear dispersive PML media by simply going through the following steps:

(1) First, as part of the initial condition, time-invariant coefficients $\Theta^L_{\rho,0}$, $\Theta^L_{\rho,1}$, $\Theta^L_{\rho,2}$, $\Theta^{NL}_{\rho,0}$, $\Theta^{NL}_{\rho,1}$, $\Theta^{NL}_{\rho,2}$ and $\Theta^{NL}_{\rho,3}$, and time-invariant matrices $\underline{\underline{\Omega_0}}$, $\underline{\underline{\Omega_1}}$, $\underline{\underline{\Omega_2}}$, $\underline{\underline{\Omega_3}}$, $\underline{\underline{\Omega_4}}$, $\underline{\underline{\Omega_5}}$, $\underline{\underline{\Omega_6}}$, $\underline{\underline{\Gamma}}^L_{\rho,0}$, $\underline{\underline{\Gamma}}^{NL}_{\rho,0}$, $\underline{\underline{\Gamma}}^{NL}_{\rho,1}$, $\underline{\underline{\Gamma}}^{NL}_{\rho,2}$, $\underline{\underline{\Gamma}}^{NL}_{\rho,3}$, $\underline{\underline{\Gamma}}^{NL}_{\rho,4}$, $\underline{\underline{\Gamma}}^{NL}_{\rho,5}$, $\underline{\underline{\Pi}}^L_{\rho,0}$, $\underline{\underline{\Pi}}^L_{\rho,1}$, $\underline{\underline{\Pi}}^L_{\rho,2}$, $\underline{\underline{\Pi}}^{NL}_{\rho,0}$, $\underline{\underline{\Pi}}^{NL}_{\rho,1}$, $\underline{\underline{\Pi}}^{NL}_{\rho,2}$, $\underline{\underline{\Pi}}^{NL}_{\rho,3}$, $\underline{\underline{\Pi}}^{NL}_{\rho,4}$, $\underline{\underline{\Pi}}^{NL}_{\rho,5}$, $\underline{\underline{\Pi}}^{NL}_{\rho,6}$ and $\underline{\underline{\Pi}}^{NL}_{\rho,7}$ are all calculated at the beginning of simulation for given values of α^L_ρ, γ^L_ρ, α^{NL}_ρ, γ^{NL}_ρ, α^L_ρ, σ_x, σ_y, σ_z and Δt. These values are stored in computer memory and used in calculating the updated field values at each time step.

(2) Using (2.44), $(\underline{H})_{ijk}^{n+\frac{1}{2}}$ is updated based on the known values of $(\underline{H})_{ijk}^{n-\frac{1}{2}}$ and $(\underline{H}^{Delay})_{ijk}^{n-\frac{1}{2}}$ and $(\underline{E})_{ijk}^{n}$.

(3) Using (2.48), $(\underline{H}^{Delay})_{ijk}^{n+\frac{1}{2}}$ is updated based on the known values of $(\underline{H}^{Delay})_{ijk}^{n-\frac{1}{2}}$, $(\underline{H})_{ijk}^{n+\frac{1}{2}}$ and $(\underline{H})_{ijk}^{n-\frac{1}{2}}$.

(4) Using (A.8) and (A.12), $\underline{\underline{(\Lambda_0)}}^n_{ijk}$ and $\underline{\underline{(\Lambda_1)}}^n_{ijk}$ are updated based on the known values of $(Q_\rho^{NL})_{ijk}^{n}$.

(5) Using (2.45), $(\underline{E})_{ijk}^{n+1}$ is updated based on the known values of $(\underline{E})_{ijk}^{n}$, $(\underline{E}^{Delay})_{ijk}^{n}$, $(Q_\rho^{L})_{ijk}^{n}$, $(Q_\rho^{LDelay})_{ijk}^{n}$ and $(\underline{H})_{ijk}^{n+\frac{1}{2}}$. Because (2.45) represents the coupled, cubic, algebraic equation, the nonlinear Newton-Raphson method[11] is used to solve for $(\underline{E})_{ijk}^{n+1}$ by finding the zero of (2.45) with the previous time step value of $(\underline{E})_{ijk}^{n}$ as the initial guess.

(6) Using (2.46), (2.47), (2.49), (2.50) and (2.51), $(\underline{Q}_\rho{}^{L})_{ijk}{}^{n+1}$, $(Q_\rho{}^{NL})_{ijk}{}^{n+1}$, $(\underline{E}^{Delay})_{ijk}{}^{n+1}$, $(\underline{Q}_\rho{}^{LDelay})_{ijk}{}^{n+1}$ and $(\underline{Q}_\rho{}^{NLDelay})_{ijk}{}^{n+1}$ are updated based on the known values of $(\underline{E})_{ijk}{}^{n+1}$, $(\underline{E})_{ijk}{}^{n}$, $(\underline{Q}_\rho{}^{L})_{ijk}{}^{n}$, $(Q_\rho{}^{NL})_{ijk}{}^{n}$, $(\underline{E}^{Delay})_{ijk}{}^{n}$, $(\underline{Q}_\rho{}^{LDelay})_{ijk}{}^{n}$ and $(\underline{Q}_\rho{}^{NLDelay})_{ijk}{}^{n}$.

(7) Increment the time step by Δt. Go back to step (2) and repeat the whole process again until the end of simulation.

Shown in Figure 1 is the flow chart of numerical steps required to update field values as described above.

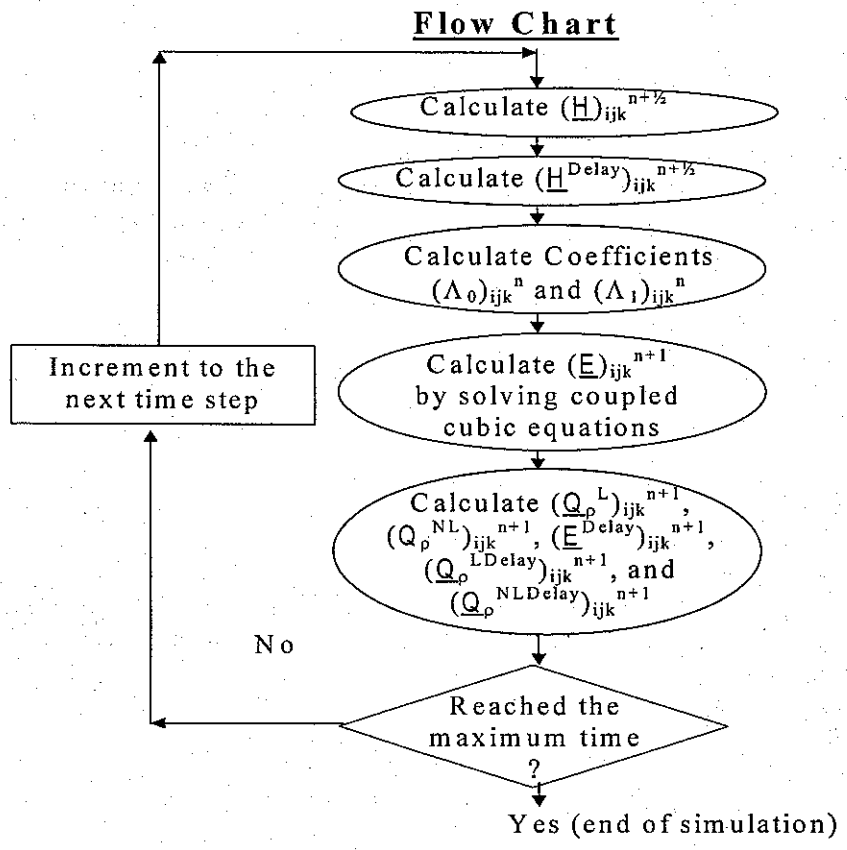

Figure 1. Flow chart of the nonlinear dispersive FDTD/PML algorithm

In the absence of the PML interface, σ_x, σ_y and σ_z can be set to zeroes. It results in reducing the nonlinear dispersive FDTD/PML algorithm to the usual nonlinear dispersive FDTD algorithm for the nonPML case.[9]

Now, if we happen to set the material coefficient α_ρ^{NL} to zero, the nonlinear dispersive FDTD/PML algorithm reduces to the linear dispersive FDTD/PML algorithm reported before.[12] Furthermore, if both α_ρ^{L} and α_ρ^{NL} are set to zeroes, it reduces to the case of the simple free space FDTD/PML algorithm.[10]

III. ONE-DIMENSIONAL FDTD/PML NUMERICAL DEMONSTRATION FOR NONLINEAR RAMAN SCATTERING MEDIA

To demonstrate the validity of the FDTD/PML algorithm, we consider the formation of a temporal soliton in one-dimensional space inside a nonlinear dispersive medium. We simulate an ultra-short optical pulse propagating into a half-space, nonlinear Raman Scattering medium, which results in the nonlinear feedback of the delayed time response to the propagating wave.[9] First, we launch an optical pulse in free space and propagate it from left to right in the positive x-direction. After traveling a short distance, the optical pulse is incident on an infinite half-space, nonlinear Raman Scattering medium that is characterized by a single first-order (linear) susceptibility function, $X_{\rho=1}^{L}(t)$, and a single third-order (nonlinear)

susceptibility function, $X^{NL}_{\rho=1}(t)$. We consider the case where $X^{L}_{\rho=1}(t)$ and $X^{NL}_{\rho=1}(t)$ are expressed in the following Lorentz forms[13,14] [i.e., set $\rho_{max} = 1$ in (2.3) for a single species]:

$$X^{(1)}_{\rho=1}(t) = \frac{\omega_0^2(\varepsilon_s - \varepsilon_R)}{\sqrt{\omega_0^2 - \delta^2}} \exp(-\delta t)\ \sin(\sqrt{\omega_0^2 - \delta^2}\ t), \tag{2.54}$$

$$X^{NL}_{\rho=1}(t) = \chi^{NL}_{01}[(\tau_1^2 + \tau_2^2)/\tau_1\ \tau_2^2]\exp(-t/\tau_2)\sin(t/\tau_1), \tag{2.55}$$

where ω_0 is the resonant frequency, ε_s is relative permittivity of a medium at DC, ε_R is the relative permittivity of a medium at infinite frequency, δ is the first-order susceptibility damping constant, χ^{NL}_{01} is the Raman Scattering strength, $1/\tau_1$ is the optical phonon frequency, and τ_2 is the optical phonon lifetime.

Comparing (2.54) and (2.55) with (2.24) and (2.25), respectively, we can relate the above coefficients to the complex coefficients, α^{L}_{ρ}, γ^{L}_{ρ}, α^{NL}_{ρ} and γ^{NL}_{ρ}, as follows:

$$\alpha^{L}_{\rho=1} \Leftarrow j\frac{\omega_0^2(\varepsilon_s - \varepsilon_R)}{\sqrt{\omega_0^2 - \delta^2}} \quad \text{and} \quad \gamma^{L}_{\rho=1} \Leftarrow (\delta + j\sqrt{\omega_0^2 - \delta^2}), \tag{2.56-2.57}$$

$$\alpha^{NL}_{\rho=1} \Leftarrow j\chi^{NL}_{01}[(\tau_1^2 + \tau_2^2)/\tau_1\ \tau_2^2] \quad \text{and} \quad \gamma^{NL}_{\rho=1} \Leftarrow (\frac{1}{\tau_2} + j\frac{1}{\tau_1}), \tag{2.58-2.59}$$

where j is the imaginary unit.

We consider the incident optical pulse to have a sinusoidal-carrier electric field frequency, ω_c, of 8.61×10^{14} radians/sec enveloped inside a hyperbolic secant function that has a width constant, T_w, of 3.50 femtoseconds. The following mathematical form describes the time-dependent incident optical pulse that we use in our one-dimensional FDTD simulation:

$$\text{Incident Optical Pulse}(t) = A\ \cos[\omega_c(t - t_{delay})]\,\text{sech}[(t - t_{delay})/T_w], \tag{2.60}$$

where A is the amplitude of the electric field and t_{delay} is the delay time for the incident optical pulse to reach its peak value. We arbitrarily assign A to take the value of 1.0 volt/meter and t_{delay} to take the value of 41.70 femtoseconds.

We select the total number of simulation cells to be 60,000, ranging from x =0 to x = 60,000, with the free-space/nonlinear-dispersive-material interface located at x = 10,000. The right-hand side of x=10,000 is represented by free space and the left-hand side of x=10,000 by the nonlinear dispersive material. We launch an optical pulse into free space at 20 cells away from the leftmost edge (at x = 20) traveling in the positive x-direction. We use the free space PML absorbing boundary condition in the left and the nonlinear PML absorbing boundary condition in the right to terminate the computational space. At both outer absorbing boundary regions, we use 10 PML cells to absorb all waves that propagate out of the computational space. Listed below are important numerical parameters and material properties that we use to perform one-dimensional FDTD/PML simulation calculations.

- Basic FDTD parameters:
  - Uniform cell size (Δx) = 5 nanometers,
  - Total simulation distance (Δx times the total number of cells) = 0.1 centimeter,
  - Time step ($\Delta t = \Delta x/2c$) = 0.00834 femtosecond, where c is the speed of light,
  - Total number of time steps = 400,000 (total simulation time = 3336 femtoseconds),
  - Quadratic increase in PML conductivities inside the PML cells.
- Linear dispersive material properties:
  - ε_s =5.25, ε_R =2.25, $\omega_o = 8.0 \times 10^{14}$ radians/second, and $\delta = 4.0 \times 10^9$ $(\text{sec})^{-1}$.
- Nonlinear dispersive material properties:
  - τ_1 = 12.2 femtoseconds, τ_2 = 32.0 femtoseconds, and χ^{NL}_{01} = 2.0 $(\text{volts/meter})^{-2}$.

By choosing 5 nanometers for Δx, we estimate the free space numerical phase velocity error[15] to be around $5x10^{-6}$, which is about the same order of accuracy as the single precision calculation of our SPARC 60 UNIX workstation.

To update the electric field value for the next time step, we use the simple Newton-Raphson iterative method[11] by making use of the current-time-step electric field value as the initial guess to solve the cubic equation. For all calculations we performed, the convergence criterion of 10^{-4} is satisfied with at most three iterations.

Figure 2 shows the time evolution of spatial electric field profiles of a delayed time response solitary wave inside the nonlinear Raman Scattering medium taken at five different time steps of 100,000Δt, 200,000Δt, 300,000Δt, 400,000Δt and 500,000Δt. As seen in this figure, at the beginning the solitary wave packet is imbedded inside the linear dispersive wave packet and it is lagged slightly behind the linear dispersive wave packet due to the nonlinear response of the Raman Scattering medium. As the wave propagates deeper into the medium, the solitary wave packet gets gradually isolated from the linear dispersive wave packet due to the slower speed of the moving solitary wave packet. By the time it reaches the time step of 300,000Δt, the solitary wave packet clearly forms its distinct solitary shape and propagates at constant amplitude while maintaining its shape. However, the shape of the solitary wave packet is uniquely different from the well-known secant function shaped wave packet that is obtained for the instantaneous time response Kerr-type case. Basically, the solitary wave packet inside the Raman Scattering medium appears retarded in time behind the linear dispersive wave packet due to the result of the nonlinear delayed time response of the medium. Details of these differences for Kerr and Raman Scattering media are discussed in Yakura *et al.*[9] Also shown Figure 2 is the efficient absorption properties of the nonlinear PML located at the rightmost edge of the computational domain. As seen in the spatial electric field profile at the time step of 500,000Δt, there is no observable reflection coming off the PML boundary.

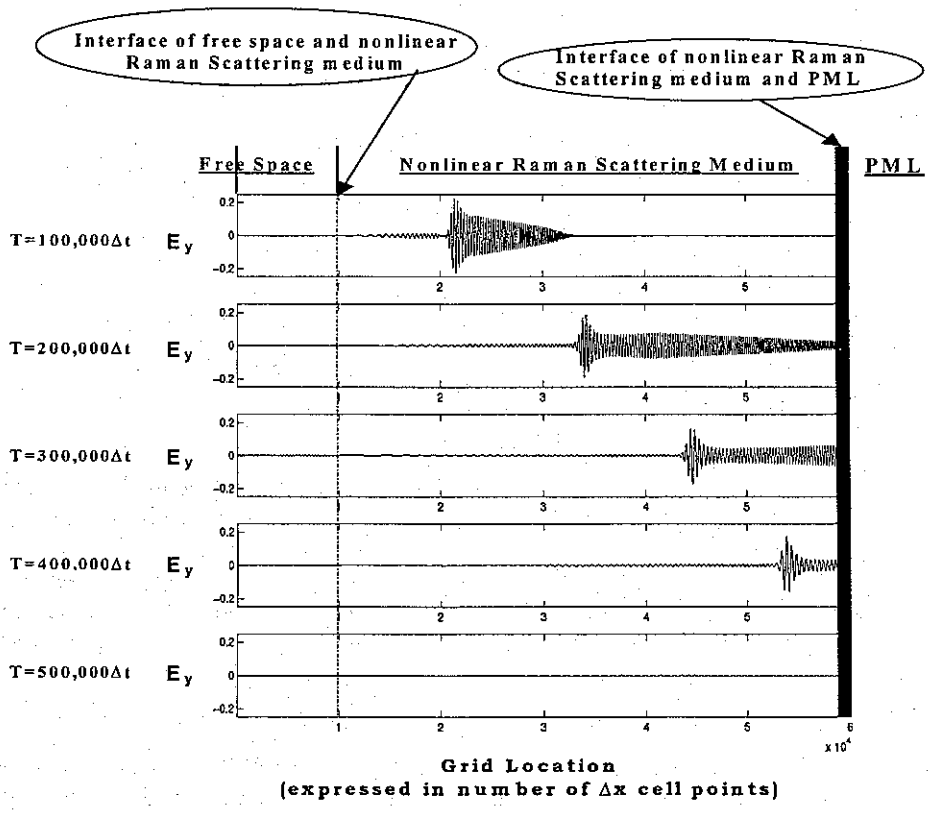

Figure 2. Comparison of spatial electric field profiles that propagate inside the nonlinear Raman Scattering medium at various time steps. The right-hand side edge is terminated by 10 cells of the nonlinear PML absorbing boundary (with $\Delta t=8.34x10^{-18}$ second and $\Delta x=5x10^{-9}$ meter). The x-axis (grid location) ranges from 0 to 60.000Δx.

To show the extent of reflection coming off the PML based on the nonlinear PML technique, we performed additional FDTD calculations using the Liao absorbing boundary condition.[16] These FDTD calculations are compared with the reference case where the interface of the absorbing boundary is extended to the right by additional 60,000 grid cells so that reflection is not important around the region of the absorbing boundary for the simulation times of interest. Figure 3 shows the comparison of the electric field profiles obtained from reference, PML absorbing boundary condition, and Liao boundary condition. As seen in Figure 3, the PML absorbing boundary condition gives good agreement with the reference case and it reveals a much better absorption property as compared to the Liao absorbing boundary condition. The maximum reflection off the nonlinear PML absorbing boundary turns out to be –19 dB as compared to –9 dB for the Liao absorbing boundary case.

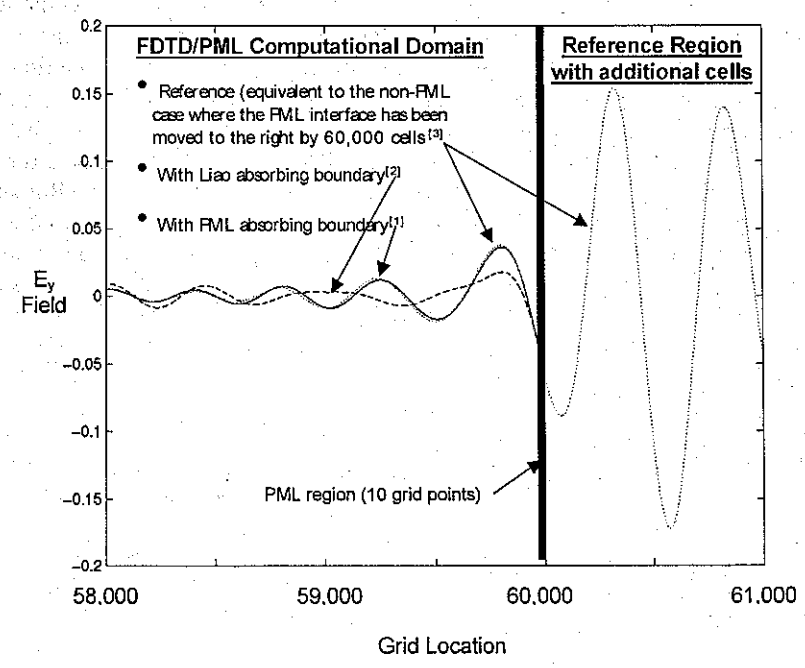

Figure 3. Comparing the spatial profiles of propagating waves at the instantaneous time step of T=450,000Δt for three different absorbing boundary conditions:
[1] Terminated the right-hand side by 10 cells of the nonlinear PML absorbing boundary,
[2] Terminated the right-hand side by the Liao absorbing boundary condition, and
[3] Extended the absorbing boundary to the right by additional 60,000 cells (The reference case with no effect of reflection).

To assure ourselves of the computational correctness of the results that we obtained from FDTD/PML algorithm, we repeated the same FDTD calculations using one-half the cell size and one-half the time step increment. These higher spatial and temporal resolution calculations resulted in a relative difference of less than 10^{-5} for the electric field value at the end of the simulation run. Since this relative difference is on the order of the single precision calculation error, we concluded that we are indeed calculating the correct electric field value. This procedure also served to validate the use of the piecewise-linear approximation.

IV. CONCLUSIONS

We present in this paper the formulation of a three-dimensional FDTD/PML algorithm inside nonlinear dispersive PML media that is used to absorb outgoing electromagnetic waves within a finite simulation volume to create the notion of infinity at the outer layer boundary of the computational volume. Because of the use of the piecewise-linear approximation, the FDTD/PML algorithm provides second-order accuracy in time for the calculation of electromagnetic field quantities. The resulting forms of the FDTD/PML algorithm tell us that we need to solve coupled cubic equations for the three components of the electric field vector at each time step due to the nonlinear behavior of the third-order electric susceptibility function.

In the absence of the nonlinear contribution, the electric field components are no longer coupled and each component of the electric field vector can be updated independently of the other two components.

For numerical validation of the FDTD/PML algorithm presented in this paper, we performed one-dimensional FDTD/PML calculations to demonstrate the efficient absorption of outgoing waves for an ultra-short optical pulse propagating inside a nonlinear Raman scattering medium with the PML absorbing boundary condition.

APPENDIX

This appendix gives the explicit expressions for coefficients and matrices used in (2.44) through (2.51). To simplify complex forms of these expressions, we first introduce the following notations in order to express them in terms of these four notations:

$$(1)\ \Psi^0[f_0(\tau)] \equiv f_0(\tau)\big|_{\tau=\Delta t}, \tag{A.1}$$

$$(2)\ \Psi^1[f_1(\tau),a_1] \equiv \int_0^{\Delta t} d\tau \left(\frac{\tau}{\Delta t}\right)^{a_1} f_1(\tau), \tag{A.2}$$

$$(3)\ \Psi^2[f_1(\tau),a_1;f_2(\tau'),a_2] \equiv \int_0^{\Delta t}\int_0^{\tau} d\tau\, d\tau' \left(\frac{\tau}{\Delta t}\right)^{a_1} f_1(\tau)\left(\frac{\tau'}{\Delta t}\right)^{a_2} f_2(\tau'), \tag{A.3}$$

$$(4)\ \Psi^3[f_1(\tau),a_1;f_2(\tau'),a_2;f_3(\tau''),a_3] \equiv \int_0^{\Delta t}\int_0^{\tau}\int_0^{\tau'} d\tau\, d\tau'\, d\tau'' \left(\frac{\tau}{\Delta t}\right)^{a_1} f_1(\tau)\left(\frac{\tau'}{\Delta t}\right)^{a_2} f_2(\tau')\left(\frac{\tau''}{\Delta t}\right)^{a_3} f_3(\tau''), \tag{A.4}$$

where $f_i(\ )$ and a_i with i=1, 2, 3 are arbitrarily defined functions and constants, respectively,

Also, we define the following three functions to be used as arguments of the above functions in which they appear frequently in representing a required form:

$$(1)\ \theta_\rho^L(\tau) \equiv \exp(-\gamma_\rho^L \tau), \tag{A.5}$$

$$(2)\ \theta_\rho^{NL}(\tau) \equiv \exp(-\gamma_\rho^{NL} \tau), \tag{A.6}$$

$$(3)\ \kappa_\eta(\tau) \equiv \exp\left(-\frac{\sigma_\eta}{\varepsilon_0}\tau\right) \text{ with } \eta = x, y, \text{ and } z. \tag{A.7}$$

In terms of notations and functions introduced above in (A.1) through (A.7), coefficients and matrices that are found in (2.44) through (2.51) [i.e., $\Theta_{\rho,0}^L$, $\Theta_{\rho,1}^L$, $\Theta_{\rho,2}^L$, $\Theta_{\rho,0}^{NL}$, $\Theta_{\rho,1}^{NL}$, $\Theta_{\rho,2}^{NL}$, $\Theta_{\rho,3}^{NL}$, $\underline{\underline{(\Lambda_0)}}_{ijk}^n$, $\underline{\underline{(\Lambda_1)}}_{ijk}^n$, $\underline{\underline{\Omega_0}}$, $\underline{\underline{\Omega_1}}$, $\underline{\underline{\Omega_2}}$, $\underline{\underline{\Omega_3}}$, $\underline{\underline{\Omega_4}}$, $\underline{\underline{\Omega_5}}$, $\underline{\underline{\Omega_6}}$, $\underline{\underline{\Gamma_{\rho,0}^L}}$, $\underline{\underline{\Gamma_{\rho,0}^{NL}}}$, $\underline{\underline{\Gamma_{\rho,1}^{NL}}}$, $\underline{\underline{\Gamma_{\rho,2}^{NL}}}$, $\underline{\underline{\Gamma_{\rho,3}^{NL}}}$, $\underline{\underline{\Gamma_{\rho,4}^{NL}}}$, $\underline{\underline{\Gamma_{\rho,5}^{NL}}}$, $\underline{\underline{\Pi_{\rho,0}^L}}$, $\underline{\underline{\Pi_{\rho,1}^L}}$, $\underline{\underline{\Pi_{\rho,2}^L}}$, $\underline{\underline{\Pi_{\rho,0}^{NL}}}$, $\underline{\underline{\Pi_{\rho,1}^{NL}}}$, $\underline{\underline{\Pi_{\rho,2}^{NL}}}$, $\underline{\underline{\Pi_{\rho,3}^{NL}}}$, $\underline{\underline{\Pi_{\rho,4}^{NL}}}$, $\underline{\underline{\Pi_{\rho,5}^{NL}}}$ and $\underline{\underline{\Pi_{\rho,6}^{NL}}}$] can be expressed as follows:

$$\Theta_{\rho,0}^L = \Psi^0[\theta_\rho^L(\tau)], \tag{A.8}$$

$$\Theta_{\rho,1}^L = \frac{\alpha_\rho^L}{\varepsilon_R}\{\Psi^1[\theta_\rho^L(\tau),0] - \Psi^1[\theta_\rho^L(\tau),1]\}, \tag{A.9}$$

$$\Theta_{\rho,2}^L = \frac{\alpha_\rho^L}{\varepsilon_R}\Psi^1[\theta_\rho^L(\tau),1], \tag{A.10}$$

$$\Theta_{\rho,0}^{NL} = \Psi^1[\theta_\rho^{NL}(\tau)], \tag{A.11}$$

$$\Theta_{\rho,1}^{NL} = \frac{\alpha_\rho^{NL}}{\varepsilon_R}\{\Psi^1[\theta_\rho^{NL}(\tau),0] - 2\Psi^1[\theta_\rho^{NL}(\tau),1] + \Psi^1[\theta_\rho^{NL}(\tau),2]\}, \tag{A.12}$$

$$\Theta_{\rho,2}^{NL} = \frac{2\alpha_\rho^{NL}}{\varepsilon_R}\{\Psi^1[\theta_\rho^{NL}(\tau),1] - \Psi^1[\theta_\rho^{NL}(\tau),2]\}, \tag{A.13}$$

$$\Theta_{\rho,3}^{NL} = \frac{\alpha_\rho^{NL}}{\varepsilon_R}\Psi^1[\theta_\rho^{NL}(\tau),2], \tag{A.14}$$

$$\underline{\underline{(\Lambda_0)}}_{ijk}^n = \text{diag}\{[(\Lambda_0)_{ijk}^n]_{11}, [(\Lambda_0)_{ijk}^n]_{22}, [(\Lambda_0)_{ijk}^n]_{33}\} \text{ with the first diagonal element expressed by} \tag{A.15}$$

$$[(\Lambda_0)^n_{ijk}]_{11} = 1+[(\frac{\sigma_y}{\varepsilon_0})+(\frac{\sigma_z}{\varepsilon_0})-(\frac{\sigma_x}{\varepsilon_0})]\frac{\Delta t}{2}+[(\frac{\sigma_y}{\varepsilon_0})-(\frac{\sigma_x}{\varepsilon_0})][(\frac{\sigma_z}{\varepsilon_0})-(\frac{\sigma_x}{\varepsilon_0})]\ \Psi^2[\kappa_x(\tau),0;\kappa_x(-\tau'),1]$$
$$+\frac{1}{\varepsilon_R}\mathrm{Re}\{\sum_\rho \alpha_\rho^L\,\Psi^0[\theta_\rho^L(\tau)]\,\Psi^1[\theta_\rho^L(\tau),1]\}$$
$$+\frac{1}{\varepsilon_R}[(\frac{\sigma_y}{\varepsilon_0})+(\frac{\sigma_z}{\varepsilon_0})-(\frac{\sigma_x}{\varepsilon_0})]\mathrm{Re}\{\sum_\rho \alpha_\rho^L\ \Psi^2[\theta_\rho^L(\tau),0;\theta_\rho^L(-\tau'),1]\}$$
$$+\frac{1}{\varepsilon_R}[(\frac{\sigma_y}{\varepsilon_0})-(\frac{\sigma_x}{\varepsilon_0})][(\frac{\sigma_z}{\varepsilon_0})-(\frac{\sigma_x}{\varepsilon_0})]\ \mathrm{Re}\{\sum_\rho \alpha_\rho^L\,\Psi^3[\kappa_x(\tau),0;\kappa_x(-\tau')\theta_\rho^L(t),0;\theta_\rho^L(-\tau''),0]\}$$
$$+\frac{1}{\varepsilon_R}\mathrm{Re}\{\sum_\rho \Psi^0[\theta_\rho^{NL}(\tau)]\,(Q_\rho^{NL})^n_{ijk}\}$$
$$+\frac{1}{\varepsilon_R}[(\frac{\sigma_y}{\varepsilon_0})+(\frac{\sigma_z}{\varepsilon_0})-(\frac{\sigma_x}{\varepsilon_0})]\mathrm{Re}\{\sum_\rho \Psi^1[\theta_\rho^{NL}(\tau),1]\,(Q_\rho^{NL})^n_{ijk}$$
$$+\frac{1}{\varepsilon_R}[(\frac{\sigma_y}{\varepsilon_0})-(\frac{\sigma_x}{\varepsilon_0})][(\frac{\sigma_z}{\varepsilon_0})-(\frac{\sigma_x}{\varepsilon_0})]\mathrm{Re}\{\sum_\rho \Psi^2[\theta_\rho^{NL}(\tau),0;\theta_\rho^{NL}(-\tau'),1]\,(Q_\rho^{NL})^n_{ijk}\},\qquad (A.16)$$

$\underline{\underline{(\Lambda_1)^n_{ijk}}} = \mathrm{diag}\{[(\Lambda_1)^n_{ijk}]_{11},[(\Lambda_1)^n_{ijk}]_{22},[(\Lambda_1)^n_{ijk}]_{33}\}$ with the first diagonal element expressed by (A.17)

$$[(\Lambda_1)^n_{ijk}]_{11} = -1+[(\frac{\sigma_y}{\varepsilon_0})+(\frac{\sigma_z}{\varepsilon_0})-(\frac{\sigma_x}{\varepsilon_0})]\frac{\Delta t}{2}$$
$$+[(\frac{\sigma_y}{\varepsilon_0})-(\frac{\sigma_x}{\varepsilon_0})][(\frac{\sigma_z}{\varepsilon_0})-(\frac{\sigma_x}{\varepsilon_0})]\ \{\Psi^2[\kappa_x(\tau),0;\kappa_x(-\tau'),0]-\Psi^2[\kappa_x(\tau),0;\kappa_x(-\tau'),1]\}$$
$$+\frac{1}{\varepsilon_R}\mathrm{Re}\{\sum_\rho \alpha_\rho^L\,\Psi^0[\theta_\rho^L(\tau)]\,\{\Psi^1[\theta_\rho^L(\tau),0]-\Psi^1[\theta_\rho^L(\tau),1]\}\}$$
$$+\frac{1}{\varepsilon_R}[(\frac{\sigma_y}{\varepsilon_0})+(\frac{\sigma_z}{\varepsilon_0})-(\frac{\sigma_x}{\varepsilon_0})]\ \mathrm{Re}\{\sum_\rho \alpha_\rho^L\ \{\Psi^2[\theta_\rho^L(\tau),0;\theta_\rho^L(-\tau'),0]-\Psi^2[\theta_\rho^L(\tau),0;\theta_\rho^L(-\tau'),1]\}$$
$$+\frac{1}{\varepsilon_R}[(\frac{\sigma_y}{\varepsilon_0})-(\frac{\sigma_x}{\varepsilon_0})][(\frac{\sigma_z}{\varepsilon_0})-(\frac{\sigma_x}{\varepsilon_0})]\ \mathrm{Re}\{\sum_\rho \alpha_\rho^L\,\{\Psi^3[\kappa_x(\tau),0;\kappa_x(-\tau')\,\theta_\rho^L(t),0;\theta_\rho^L(-\tau''),0]$$
$$-\Psi^3[\kappa_x(\tau),0;\kappa_x(-\tau')\theta_\rho^L(t),0;\theta_\rho^L(-\tau''),1]\}\}$$
$$-\frac{1}{\varepsilon_R}\mathrm{Re}\{\sum_\rho (Q_\rho^{NL})^n_{ijk}\}$$
$$+\frac{1}{\varepsilon_R}[(\frac{\sigma_y}{\varepsilon_0})+(\frac{\sigma_z}{\varepsilon_0})-(\frac{\sigma_x}{\varepsilon_0})]\ \mathrm{Re}\{\sum_\rho \{\Psi^1[\theta_\rho^{NL}(\tau),0]-\Psi^1[\theta_\rho^{NL}(\tau),1]\}\,(Q_\rho^{NL})^n_{ijk}\}$$
$$+\frac{1}{\varepsilon_R}[(\frac{\sigma_y}{\varepsilon_0})-(\frac{\sigma_x}{\varepsilon_0})][(\frac{\sigma_z}{\varepsilon_0})-(\frac{\sigma_x}{\varepsilon_0})]$$
$$\cdot\mathrm{Re}\{\sum_\rho \{\Psi^2[\theta_\rho^{NL}(\tau),0;\theta_\rho^{NL}(-\tau'),0]-\Psi^2[\theta_\rho^{NL}(\tau),0;\theta_\rho^{NL}(-\tau'),1]\}\,(Q_\rho^{NL})^n_{ijk}\},\qquad (A.18)$$

$\underline{\underline{\Omega_0}} = \mathrm{diag}\{(\Omega_0)_{11},(\Omega_0)_{22},(\Omega_0)_{33}\}$ with the first diagonal element given by (A.19)

$$(\Omega_0)_{11} = 1+[(\frac{\sigma_y}{\varepsilon_0})+(\frac{\sigma_z}{\varepsilon_0})-(\frac{\sigma_x}{\varepsilon_0})]\frac{\Delta t}{2}+[(\frac{\sigma_y}{\varepsilon_0})-(\frac{\sigma_x}{\varepsilon_0})][(\frac{\sigma_z}{\varepsilon_0})-(\frac{\sigma_x}{\varepsilon_0})]\ \Psi^2[\kappa_x(\tau),0;\kappa_x(-\tau'),1],\qquad (A.20)$$

$\underline{\underline{\Omega_1}} = \mathrm{diag}\{(\Omega_1)_{11},(\Omega_1)_{22},(\Omega_1)_{33}\}$ with the first diagonal element given by (A.21)

$$(\Omega_1)_{11} = -1 + [(\frac{\sigma_y}{\varepsilon_0}) + (\frac{\sigma_z}{\varepsilon_0}) - (\frac{\sigma_x}{\varepsilon_0})]\frac{\Delta t}{2}$$
$$+ [(\frac{\sigma_y}{\varepsilon_0}) - (\frac{\sigma_x}{\varepsilon_0})][(\frac{\sigma_z}{\varepsilon_0}) - (\frac{\sigma_x}{\varepsilon_0})]\{\Psi^2[\kappa_x(\tau),0;\kappa_x(-\tau'),0] - \Psi^2[\kappa_x(\tau),0;\kappa_x(-\tau'),1]\}, \quad (A.22)$$

$\underline{\underline{\Omega_2}} = \text{diag}\{(\Omega_2)_{11},(\Omega_2)_{22},(\Omega_2)_{33}\}$ with the first diagonal element given by (A.23)

$$(\Omega_2)_{11} = [(\frac{\sigma_y}{\varepsilon_0}) - (\frac{\sigma_x}{\varepsilon_0})][(\frac{\sigma_z}{\varepsilon_0}) - (\frac{\sigma_x}{\varepsilon_0})]\,\Psi^1[\kappa_x(\tau),0], \quad (A.24)$$

$$\underline{\underline{\Omega_3}} = \frac{1}{\varepsilon_R}\text{diag}\{(\Omega_2)_{11},(\Omega_2)_{22},(\Omega_2)_{33}\}, \quad (A.25)$$

$$\underline{\underline{\Omega_4}} = \text{diag}\{\Psi^0[\kappa_x(\tau)],\Psi^0[\kappa_y(\tau),0],\Psi^0[\kappa_z(\tau)]\}, \quad (A.26)$$

$\underline{\underline{\Omega_5}} = \text{diag}\{(\Omega_5)_{11},(\Omega_5)_{22},(\Omega_5)_{33}\}$ with the first diagonal element given by (A.27)

$$(\Omega_5)_{11} = \Psi^1[\kappa_x(\tau),0] - \Psi^1[\kappa_x(\tau),1], \quad (A.28)$$

$$\underline{\underline{\Omega_6}} = \text{diag}\{\Psi^1[\kappa_x(\tau),1],\Psi^1[\kappa_y(\tau),1],\Psi^1[\kappa_z(\tau),1]\}, \quad (A.29)$$

$\underline{\underline{\Gamma^L_{\rho,0}}} = \text{diag}\{(\Gamma^L_{\rho,0})_{11},(\Gamma^L_{\rho,0})_{22},(\Gamma^L_{\rho,0})_{33}\}$ with the first diagonal element given by (A.30)

$$(\Gamma^L_{\rho,0})_{11} = -1 + \Psi^1[\theta^L_\rho(\tau)] + [\,(\frac{\sigma_y}{\varepsilon_0}) + (\frac{\sigma_z}{\varepsilon_0}) - (\frac{\sigma_x}{\varepsilon_0})\,]\,\Psi^1[\theta^L_\rho(\tau),0]$$
$$+ [(\frac{\sigma_y}{\varepsilon_0}) - (\frac{\sigma_x}{\varepsilon_0})][(\frac{\sigma_z}{\varepsilon_0}) - (\frac{\sigma_x}{\varepsilon_0})]\,\Psi^2[\kappa_x(\tau),0;\kappa_x(-\tau')\theta^L_\rho(\tau'),0], \quad (A.31)$$

$\underline{\underline{\Gamma^{NL}_{\rho,0}}} = \frac{\alpha^{NL}_\rho}{\varepsilon_R}\text{diag}\{(\Gamma^{NL}_{\rho,0})_{11},(\Gamma^{NL}_{\rho,0})_{22},(\Gamma^{NL}_{\rho,0})_{33}\}$ with the first diagonal element given by (A.32)

$$(\Gamma^{NL}_{\rho,0})_{11} = [\,(\frac{\sigma_y}{\varepsilon_0}) + (\frac{\sigma_z}{\varepsilon_0}) - (\frac{\sigma_x}{\varepsilon_0})\,]\{\Psi^2[\theta^{NL}_\rho(\tau),0;\theta^{NL}_\rho(-\tau'),0] - 3\Psi^2[\theta^{NL}_\rho(\tau),0;\theta^{NL}_\rho(-\tau'),1]$$
$$+ 3\Psi^2[\theta^{NL}_\rho(\tau),0;\theta^{NL}_\rho(-\tau'),2] - \Psi^2[\theta^{NL}_\rho(\tau),0;\theta^{NL}_\rho(-\tau'),3]\}$$
$$+ [(\frac{\sigma_y}{\varepsilon_0}) - (\frac{\sigma_x}{\varepsilon_0})][(\frac{\sigma_z}{\varepsilon_0}) - (\frac{\sigma_x}{\varepsilon_0})]$$
$$\cdot\{\Psi^3[\kappa_x(\tau),0;\kappa_x(-\tau')\theta^{NL}_\rho(\tau'),0;\theta^{NL}_\rho(-\tau''),0] - 2\,\Psi^3[\kappa_x(\tau),0;\kappa_x(-\tau')\theta^{NL}_\rho(t),0;\theta^{NL}_\rho(-\tau''),1]$$
$$+ \Psi^3[\kappa_x(\tau),0;\kappa_x(-\tau')\theta^{NL}_\rho(\tau'),0;\theta^{NL}_\rho(-\tau''),2] - \Psi^3[\kappa_x(\tau),0;\kappa_x(-\tau')\theta^{NL}_\rho(\tau'),1;\theta^{NL}_\rho(-\tau''),0]$$
$$- 2\,\Psi^3[\kappa_x(\tau),0;\kappa_x(-\tau')\theta^{NL}_\rho(\tau'),1;\theta^{NL}_\rho(-\tau''),1] + \Psi^3[\kappa_x(\tau),0;\kappa_x(-\tau')\theta^{NL}_\rho(\tau'),1;\theta^{NL}_\rho(-\tau''),2]\}, \quad (A.33)$$

$\underline{\underline{\Gamma^{NL}_{\rho,1}}} = \frac{\alpha^{NL}_\rho}{\varepsilon_R}\text{diag}\{(\Gamma^{NL}_{\rho,1})_{11},(\Gamma^{NL}_{\rho,1})_{22},(\Gamma^{NL}_{\rho,1})_{33}\}$ with the first diagonal element given by (A.34)

$$(\Gamma^{NL}_{\rho,1})_{11} = [\,(\frac{\sigma_y}{\varepsilon_0}) + (\frac{\sigma_z}{\varepsilon_0}) - (\frac{\sigma_x}{\varepsilon_0})\,]$$
$$\cdot\{2\Psi^2[\theta^{NL}_\rho(\tau),0;\theta^{NL}_\rho(-\tau'),1] - 4\Psi^2[\theta^{NL}_\rho(\tau),0;\theta^{NL}_\rho(-\tau'),2] + 2\Psi^2[\theta^{NL}_\rho(\tau),0;\theta^{NL}_\rho(-\tau'),3]\}$$
$$+ 2[(\frac{\sigma_y}{\varepsilon_0}) - (\frac{\sigma_x}{\varepsilon_0})][(\frac{\sigma_z}{\varepsilon_0}) - (\frac{\sigma_x}{\varepsilon_0})]$$
$$\cdot\{\Psi^3[\kappa_x(\tau),0;\kappa_x(-\tau')\theta^{NL}_\rho(\tau'),0;\theta^{NL}_\rho(-\tau''),1] - \Psi^3[\kappa_x(\tau),0;\kappa_x(-\tau')\theta^{NL}_\rho(\tau'),0;\theta^{NL}_\rho(-\tau''),2]$$
$$- \Psi^3[\kappa_x(\tau),0;\kappa_x(-\tau')\theta^{NL}_\rho(\tau'),1;\theta^{NL}_\rho(-\tau''),1] + \Psi^3[\kappa_x(\tau),0;\kappa_x(-\tau')\theta^{NL}_\rho(\tau'),1;\theta^{NL}_\rho(-\tau''),2]\}, \quad (A.35)$$

$\underline{\underline{\Gamma^{NL}_{\rho,2}}} = \frac{\alpha^{NL}_\rho}{\varepsilon_R}\text{diag}\{(\Gamma^{NL}_{\rho,2})_{11},(\Gamma^{NL}_{\rho,2})_{22},(\Gamma^{NL}_{\rho,2})_{33}\}$ with the first diagonal element given by (A.36)

$$(\Gamma^{NL}_{\rho,2})_{11} = [\,(\frac{\sigma_y}{\varepsilon_0}) + (\frac{\sigma_z}{\varepsilon_0}) - (\frac{\sigma_x}{\varepsilon_0})\,]$$
$$\cdot\{\Psi^3[\kappa_x(\tau),0;\kappa_x(-\tau')\theta^{NL}_\rho(\tau'),0;\theta^{NL}_\rho(-\tau''),1] - \Psi^3[\kappa_x(\tau),0;\kappa_x(-\tau')\theta^{NL}_\rho(\tau'),0;\theta^{NL}_\rho(-\tau''),2]\}$$
$$+[(\frac{\sigma_y}{\varepsilon_0}) - (\frac{\sigma_x}{\varepsilon_0})][(\frac{\sigma_z}{\varepsilon_0}) - (\frac{\sigma_x}{\varepsilon_0})]$$
$$\cdot\{\Psi^3[\kappa_x(\tau),0;\kappa_x(-\tau')\theta^{NL}_\rho(\tau'),0;\theta^{NL}_\rho(-\tau''),3] - \Psi^3[\kappa_x(\tau),0;\kappa_x(-\tau')\theta^{NL}_\rho(\tau'),1;\theta^{NL}_\rho(-\tau''),2]\}\,, \quad (A.37)$$

$\underline{\underline{\Gamma^{NL}_{\rho,3}}} = \frac{\alpha^{NL}_\rho}{\varepsilon_R}\,\mathrm{diag}\{(\Gamma^{NL}_{\rho,3})_{11},(\Gamma^{NL}_{\rho,3})_{22},(\Gamma^{NL}_{\rho,3})_{33}\}$ with the first diagonal element given by (A.38)

$$(\Gamma^{NL}_{\rho,3})_{11} = \Psi^0[\theta^{NL}_\rho(\tau)]\,\{\Psi^1[\theta^{NL}_\rho(\tau),0] - 2\,\Psi^1[\theta^{NL}_\rho(\tau),1] + \Psi^1[\theta^{NL}_\rho(\tau),2]\}$$
$$+[\,(\frac{\sigma_y}{\varepsilon_0}) + (\frac{\sigma_z}{\varepsilon_0}) - (\frac{\sigma_x}{\varepsilon_0})\,]$$
$$\cdot\{\Psi^2[\theta^{NL}_\rho(\tau),0;\theta^{NL}_\rho(-\tau'),1] - 2\Psi^2[\theta^{NL}_\rho(\tau),0;\theta^{NL}_\rho(-\tau'),2] + \Psi^2[\theta^{NL}_\rho(\tau),0;\theta^{NL}_\rho(-\tau'),3]\}$$
$$+[(\frac{\sigma_y}{\varepsilon_0}) - (\frac{\sigma_x}{\varepsilon_0})][(\frac{\sigma_z}{\varepsilon_0}) - (\frac{\sigma_x}{\varepsilon_0})]$$
$$\cdot\{\Psi^3[\kappa_x(\tau),0;\kappa_x(-\tau')\theta^{NL}_\rho(\tau'),1;\theta^{NL}_\rho(-\tau''),0] - 2\,\Psi^3[\kappa_x(\tau),0;\kappa_x(-\tau')\theta^{NL}_\rho(\tau'),1;\theta^{NL}_\rho(-\tau''),1]$$
$$+\,\Psi^3[\kappa_x(\tau),0;\kappa_x(-\tau')\theta^{NL}_\rho(\tau'),1;\theta^{NL}_\rho(-\tau''),2]\}\,, \quad (A.39)$$

$\underline{\underline{\Gamma^{NL}_{\rho,4}}} = \frac{\alpha^{NL}_\rho}{\varepsilon_R}\,\mathrm{diag}\{(\Gamma^{NL}_{\rho,4})_{11},(\Gamma^{NL}_{\rho,4})_{22},(\Gamma^{NL}_{\rho,4})_{33}\}$ with the first diagonal element given by (A.40)

$$(\Gamma^{NL}_{\rho,4})_{11} = 2\Psi^0[\theta^{NL}_\rho(\tau)]\,\{\Psi^1[\theta^{NL}_\rho(\tau),1] - \Psi^1[\theta^{NL}_\rho(\tau),2]\}$$
$$+2\,[\,(\frac{\sigma_y}{\varepsilon_0}) + (\frac{\sigma_z}{\varepsilon_0}) - (\frac{\sigma_x}{\varepsilon_0})\,]\,\{\Psi^2[\theta^{NL}_\rho(\tau),0;\theta^{NL}_\rho(-\tau'),2] - \Psi^2[\theta^{NL}_\rho(\tau),0;\theta^{NL}_\rho(-\tau'),3]\}$$
$$+2\,[(\frac{\sigma_y}{\varepsilon_0}) - (\frac{\sigma_x}{\varepsilon_0})][(\frac{\sigma_z}{\varepsilon_0}) - (\frac{\sigma_x}{\varepsilon_0})]$$
$$\cdot\{\Psi^3[\kappa_x(\tau),0;\kappa_x(-\tau')\theta^{NL}_\rho(\tau'),1;\theta^{NL}_\rho(-\tau''),1] - \Psi^3[\kappa_x(\tau),0;\kappa_x(-\tau')\theta^{NL}_\rho(\tau'),1;\theta^{NL}_\rho(-\tau''),2]\}\,, \quad (A.41)$$

$\underline{\underline{\Gamma^{NL}_{\rho,5}}} = \frac{\alpha^{NL}_\rho}{\varepsilon_R}\,\mathrm{diag}\{(\Gamma^{NL}_{\rho,5})_{11},(\Gamma^{NL}_{\rho,5})_{22},(\Gamma^{NL}_{\rho,5})_{33}\}$ with the first diagonal element given by (A.42)

$$(\Gamma^{NL}_{\rho,5})_{11} = \Psi^0[\theta^{NL}_\rho(\tau)]\,\Psi^1[\theta^{NL}_\rho(\tau),2] + [\,(\frac{\sigma_y}{\varepsilon_0}) + (\frac{\sigma_z}{\varepsilon_0}) - (\frac{\sigma_x}{\varepsilon_0}) - (\gamma^{NL}_\rho)\,]\,\Psi^2[\theta^{NL}_\rho(\tau),0;\theta^{NL}_\rho(-\tau'),3]$$
$$+[(\frac{\sigma_y}{\varepsilon_0}) - (\frac{\sigma_x}{\varepsilon_0})][(\frac{\sigma_z}{\varepsilon_0}) - (\frac{\sigma_x}{\varepsilon_0})]\,\Psi^3[\kappa_x(\tau),0;\kappa_x(-\tau')\theta^{NL}_\rho(\tau'),1;\theta^{NL}_\rho(-\tau''),2]\,, \quad (A.43)$$

$\underline{\underline{\Pi^{L}_{\rho,0}}} = \frac{\alpha^{L}_\rho}{\varepsilon_R}\,\mathrm{diag}\{(\Pi^{L}_{\rho,0})_{11},(\Pi^{L}_{\rho,0})_{22},(\Pi^{L}_{\rho,0})_{33}\}$ with the first diagonal element given by (A.44)

$$(\Gamma^{L}_{\rho,0})_{11} = \Psi^1[\kappa_x(-\tau)\theta^{L}_\rho(\tau),0]\,, \quad (A.45)$$

$\underline{\underline{\Pi^{L}_{\rho,1}}} = \frac{\alpha^{L}_\rho}{\varepsilon_R}\,\mathrm{diag}\{(\Pi^{L}_{\rho,1})_{11},(\Pi^{L}_{\rho,1})_{22},(\Pi^{L}_{\rho,1})_{33}\}$ with the first diagonal element given by (A.46)

$$(\Gamma^{L}_{\rho,1})_{11} = \Psi^2[\kappa_x(-\tau)\theta^{L}_\rho(\tau),0;\theta^{L}_\rho(-\tau'),0] - \Psi^2[\kappa_x(-\tau)\theta^{L}_\rho(\tau),0;\theta^{L}_\rho(-\tau'),1]\,, \quad (A.47)$$

$\underline{\underline{\Pi^{L}_{\rho,2}}} = \frac{\alpha^{L}_\rho}{\varepsilon_R}\,\mathrm{diag}\{(\Pi^{L}_{\rho,2})_{11},(\Pi^{L}_{\rho,2})_{22},(\Pi^{L}_{\rho,2})_{33}\}$ with the first diagonal element given by (A.48)

$$(\Gamma^{L}_{\rho,2})_{11} = \Psi^2[\kappa_x(-\tau)\theta^{L}_\rho(\tau),0;\theta^{L}_\rho(-\tau'),1]\,, \quad (A.49)$$

$\underline{\underline{\Pi^{NL}_{\rho,0}}} = \frac{\alpha^{NL}_\rho}{\varepsilon_R}\,\mathrm{diag}\{(\Pi^{NL}_{\rho,0})_{11},(\Pi^{NL}_{\rho,0})_{22},(\Pi^{NL}_{\rho,0})_{33}\}$ with the first diagonal element given by (A.50)

$$(\Pi^{NL}_{\rho,0})_{11} = \Psi^1[\kappa_x(-\tau)\theta^{NL}_\rho(\tau),0] - \Psi^1[\kappa_x(-\tau)\theta^{NL}_\rho(\tau),1]\,, \quad (A.51)$$

$$\underline{\underline{\Pi}}^{NL}_{\rho,1} = \frac{\alpha^{NL}_{\rho}}{\varepsilon_R}\,\mathrm{diag}\left\{(\Pi^{NL}_{\rho,1})_{11},(\Pi^{NL}_{\rho,1})_{22},(\Pi^{NL}_{\rho,1})_{33}\right\} \text{ with the first diagonal element given by} \tag{A.52}$$

$$(\Pi^{NL}_{\rho,1})_{11} = \Psi^1[\kappa_x(-\tau)\theta^{NL}_{\rho}(\tau),1], \tag{A.53}$$

$$\underline{\underline{\Pi}}^{NL}_{\rho,2} = \frac{\alpha^{NL}_{\rho}}{\varepsilon_R}\,\mathrm{diag}\left\{(\Pi^{NL}_{\rho,2})_{11},(\Pi^{NL}_{\rho,2})_{22},(\Pi^{NL}_{\rho,2})_{33}\right\} \text{ with the first diagonal element given by} \tag{A.54}$$

$$\begin{aligned}(\Pi^{NL}_{\rho,2})_{11} = {} & \Psi^2[\kappa_x(-\tau)\theta^{NL}_{\rho}(\tau),0;\theta^{NL}_{\rho}(-\tau'),0] - 2\,\Psi^2[\kappa_x(-\tau)\theta^{L}_{\rho}(\tau),0;\theta^{L}_{\rho}(-\tau'),1] \\ & + \Psi^2[\kappa_x(-\tau)\theta^{NL}_{\rho}(\tau),0;\theta^{NL}_{\rho}(-\tau'),2] - \Psi^2[\kappa_x(-\tau)\theta^{NL}_{\rho}(\tau),1;\theta^{NL}_{\rho}(-\tau'),0] \\ & + 2\Psi^2[\kappa_x(-\tau)\theta^{NL}_{\rho}(\tau),1;\theta^{NL}_{\rho}(-\tau'),1] - \Psi^2[\kappa_x(-\tau)\theta^{NL}_{\rho}(\tau),1;\theta^{NL}_{\rho}(-\tau'),2],\end{aligned} \tag{A.55}$$

$$\underline{\underline{\Pi}}^{NL}_{\rho,3} = \frac{\alpha^{NL}_{\rho}}{\varepsilon_R}\,\mathrm{diag}\left\{(\Pi^{NL}_{\rho,3})_{11},(\Pi^{NL}_{\rho,3})_{22},(\Pi^{NL}_{\rho,3})_{33}\right\} \text{ with the first diagonal element given by} \tag{A.56}$$

$$\begin{aligned}(\Pi^{NL}_{\rho,3})_{11} = {} & \Psi^2[\kappa_x(-\tau)\theta^{L}_{\rho}(\tau),0;\theta^{L}_{\rho}(-\tau'),1] - 2\,\Psi^2[\kappa_x(-\tau)\theta^{L}_{\rho}(\tau),0;\theta^{L}_{\rho}(-\tau'),2] \\ & - 2\,\Psi^2[\kappa_x(-\tau)\theta^{NL}_{\rho}(\tau),1;\theta^{NL}_{\rho}(-\tau'),1] + \Psi^2[\kappa_x(-\tau)\theta^{NL}_{\rho}(\tau),1;\theta^{NL}_{\rho}(-\tau'),2],\end{aligned} \tag{A.57}$$

$$\underline{\underline{\Pi}}^{NL}_{\rho,4} = \frac{\alpha^{NL}_{\rho}}{\varepsilon_R}\,\mathrm{diag}\left\{(\Pi^{NL}_{\rho,4})_{11},(\Pi^{NL}_{\rho,4})_{22},(\Pi^{NL}_{\rho,4})_{33}\right\} \text{ with the first diagonal element given by} \tag{A.58}$$

$$(\Pi^{NL}_{\rho,4})_{11} = \Psi^2[\kappa_x(-\tau)\theta^{NL}_{\rho}(\tau),1;\theta^{NL}_{\rho}(-\tau'),0] - \Psi^2[\kappa_x(-\tau)\theta^{NL}_{\rho}(\tau),1;\theta^{NL}_{\rho}(-\tau'),2], \tag{A.59}$$

$$\underline{\underline{\Pi}}^{NL}_{\rho,5} = \frac{\alpha^{NL}_{\rho}}{\varepsilon_R}\,\mathrm{diag}\left\{(\Pi^{NL}_{\rho,5})_{11},(\Pi^{NL}_{\rho,5})_{22},(\Pi^{NL}_{\rho,5})_{33}\right\} \text{ with the first diagonal element given by} \tag{A.60}$$

$$\begin{aligned}(\Pi^{NL}_{\rho,5})_{11} = {} & \Psi^2[\kappa_x(-\tau)\theta^{NL}_{\rho}(\tau),1;\theta^{NL}_{\rho}(-\tau'),0] - 2\,\Psi^2[\kappa_x(-\tau)\theta^{NL}_{\rho}(\tau),1;\theta^{NL}_{\rho}(-\tau'),1] \\ & + \Psi^2[\kappa_x(-\tau)\theta^{NL}_{\rho}(\tau),1;\theta^{NL}_{\rho}(-\tau'),2],\end{aligned} \tag{A.61}$$

$$\underline{\underline{\Pi}}^{NL}_{\rho,6} = \frac{\alpha^{NL}_{\rho}}{\varepsilon_R}\,\mathrm{diag}\left\{(\Pi^{NL}_{\rho,6})_{11},(\Pi^{NL}_{\rho,6})_{22},(\Pi^{NL}_{\rho,6})_{33}\right\} \text{ with the first diagonal element given by} \tag{A.62}$$

$$(\Pi^{NL}_{\rho,6})_{11} = 2\left\{\Psi^2[\kappa_x(-\tau)\theta^{NL}_{\rho}(\tau),1;\theta^{NL}_{\rho}(-\tau'),1] - \Psi^2[\kappa_x(-\tau)\theta^{NL}_{\rho}(\tau),1;\theta^{NL}_{\rho}(-\tau'),2]\right\}, \tag{A.63}$$

$$\underline{\underline{\Pi}}^{NL}_{\rho,7} = \frac{\alpha^{NL}_{\rho}}{\varepsilon_R}\,\mathrm{diag}\left\{(\Pi^{NL}_{\rho,7})_{11},(\Pi^{NL}_{\rho,7})_{22},(\Pi^{NL}_{\rho,7})_{33}\right\} \text{ with the first diagonal element given by} \tag{A.64}$$

$$(\Pi^{NL}_{\rho,7})_{11} = \Psi^2[\kappa_x(-\tau)\theta^{NL}_{\rho}(\tau),1;\theta^{NL}_{\rho}(-\tau'),2]. \tag{A.65}$$

For all the above matrices, the second diagonal element is obtained simply by replacing the indices as follows: [x→y, y→z, and z→x]. Similarly, the third diagonal element is obtained simply by replacing the indices as follows: [x→z, y→x, and z→y].

As noted before, the above coefficients and matrices can be evaluated explicitly in terms of the known values Δt, α^L_ρ, γ^L_ρ, α^{NL}_ρ, γ^{NL}_ρ, σ_x, σ_y and σ_z before the start of simulation.

REFERENCES

1. K. S. Yee, "Numerical Solution of Initial Boundary Value Problems Involving Maxwell's Equations in Isotropic Media," IEEE Trans. Antennas and Propagation, Vol. 14, pp. 302-307, 1966.
2. J. P. Berenger, "A Perfectly Matched Layer for the Absorption of Electromagnetic Waves," J. Computational Physics, Vol. 114, pp. 185-200, 1994.
3. W. C. Chew, W. Weeden, " A 3D Perfectly Matched Medium from Modified Maxwell's Equations with Stretched Coordinates," Microwave Opt. Tech. Letter, Vol. 7, pp. 599-604, 1994.
4. Z. S. Sacks, D. M. Kingsland, R. Lee, J. F. Lee, "A Perfectly Matched Anisotropic Absorber for Use as an Absorbing Boundary Condition," IEEE Trans. Antennas and Propagation, Vol. 43, pp. 1460-1463, 1995.
5. S. D. Gedney, "An Anisotropic PML Absorbing Media for FDTD Simulation of Fields in Lossy Dispersive Media," Electromagnetics, Vol. 16, pp. 399-415, 1996.
6. S. D. Gedney, "An Anisotropic Perfectly Matched Layer Absorbing Media for the Truncation of FDTD Lattices," IEEE Trans. Antennas and Propagation, Vol. 44, pp. 1630-1639, 1996.

7. A. Taflove, *Advances in Computational Electromagnetics: The Finite-Difference Time-Domain Method*, Chapter 5, Artech House, 1998.
8. F. L. Teixeira, W. C. Chew, M. L. Oristaglio, T. Wang, " Perfectly Matched Layer and Piecewise-linear Recursive Convolution for the FDTD Solution of the 3D Dispersive Half-space Problem," IEEE Trans. On Magnetics, Vol. 34, pp. 2247-2250, 1998.
9. S. J. Yakura, J. T. MacGillivray, D. Dietz, "A Three-dimensional Finite-Difference Time-Domain Algorithm Based on the Recursive Convolution Approach for Propagation of Electromagnetic Waves in Nonlinear Dispersive Media," Applied Computational Electromagnetic Society (ACES) Journal, Vol. 16, No. 1, pp. 33-44, March 2001.
10. S. J. Yakura, D. Dietz, A. D. Greenwood, "A Dynamic Stability Analysis of the PML Method," Submitted to IEEE Trans. Antennas and Propagation in March 2001.
11. W. H. Press, S. A. Teukolsky, W. T. Vetterling and B. P. Flannery, "Numerical Recipes in FORTRAN - The Art of Scientific Computing, Second Edition," Chapter 9: Root Finding and Nonlinear Sets of Equations, pp. 372-375, Cambridge University Press, 1992.
12. S. J. Yakura, D. Dietz, "A Three-dimensional Finite Difference Time Domain – Perfectly Matched Layer Algorithm Based On Piecewise-linear Approximation For Linear Dispersive Media," US Air Force Technical Report AFRL-DE-TR-2000-1013, Kirtland AFB, NM, February 2000.
13. P. M. Goorjian, A. Taflove, R. M. Joseph, S. C. Hagness, "Computational Modeling of Femtosecond Optical Solitons from Maxwell's Equations," IEEE J. of Quantum Electronics, Vol. 28, pp. 2416-2422, 1992.
14. P. M. Goorjian, A. Taflove, "Direct Time Integration of Maxwell's Equations in Nonlinear Dispersive Media for Propagation of Femtosecond Electromagnetic Solitons," Opt. Lett., Vol. 17, pp. 180-182, 1992.
15. A. Taflove, *Computational Electromagnetics: The Finite-Difference Time-Domain Method*, pp. 42-44, Artech House, 1995.
16. Z. P. Liao, H. L. Wong, B. P. Yang, Y. F. Yuan, "A Transmitting Boundary for Transient Wave Analysis," Scientia Sinica, Vol. XXVII, pp. 1063-1076, 1984.